NASA Contractor Report 159372

EFFECTS OF BOUNDARY-LAYER TREATMENT ON CRYOGENIC WIND-TUNNEL CONTROLS

S. Balakrishna

OLD DOMINION UNIVERSITY
Norfolk, Virginia 23508

NASA Grant NSG-1503
August 1980

NASA
National Aeronautics and Space Administration
Langley Research Center
Hampton, Virginia 23665

DEPARTMENT OF MECHANICAL ENGINEERING AND MECHANICS
SCHOOL OF ENGINEERING
OLD DOMINION UNIVERSITY
NORFOLK, VIRGINIA

EFFECTS OF BOUNDARY-LAYER TREATMENT ON CRYOGENIC WIND-TUNNEL CONTROLS

By

S. Balakrishna

Principal Investigator: G.L. Goglia

Progress Report
For the period ending August 1980

Prepared for the
National Aeronautics and Space Administration
Langley Research Center
Hampton, Virginia 23665

Under
Research Grant NSG 1503
Dr. Robert A. Kilgore, Technical Monitor
Subsonic Transonic Aerodynamics Division

Submitted by the
Old Dominion University Research Foundation
P.O. Box 6369
Norfolk, Virginia 23508

August 1980

PREFACE

This report analyzes the manner in which various possible schemes for sidewall boundary-layer treatment, that can be used to achieve a two-dimensional flow field around the model in the 0.3-meter Transonic Cryogenic Tunnel Facility, affect the basic tunnel controls. This work constitutes a part of the project "Modeling and Control of Transonic Cryogenic Tunnels" sponsored by NASA/Langley Research Center (LaRC) under research grant NSG 1503. The contents of this document complement other reports on the project: on modeling phase activity (reported in reference 1), control analysis phase activity (reported in reference 2), and the test direction analysis (reported in reference 3).

TABLE OF CONTENTS

	Page
PREFACE	ii
INTRODUCTION	1
NOMENCLATURE	2
CRYOGENIC TUNNEL UNDER EQUILIBRIUM	4
BOUNDARY-LAYER TREATMENT SCHEMES	5
BOUNDARY-LAYER BLEED MASS FLOW MANAGEMENT	7
PASSIVE BOUNDARY-LAYER BLEED CONTROL	8
RECIRCULATION MODE BOUNDARY-LAYER CONTROL	14
ENGINEERING CONSIDERATIONS FOR VARIOUS BOUNDARY-LAYER TREATMENT SCHEMES	16
SUMMARY AND CONCLUDING REMARKS	23
APPENDIX	25
REFERENCES	32
FIGURES	33

LIST OF FIGURES

Figure		
1	Configuration of the 0.3-m TCT	33
2	Thermodynamic model of a cryogenic tunnel	34
3	Energy state diagram	35
4	Test section and boundary-layer removal valves	36
5	Loci of boundary-layer bleed mass flow, 100 K	37
6	Loci of boundary-layer bleed mass flow, 200 K	38
7	Loci of boundary-layer bleed mass flow, 300 K	39

LIST OF FIGURES - CONCLUDED

Figure		Page
8	Minimum tunnel pressure required for passive boundary-layer bleed mode of operation	40
9	Loci of energy required for balanced cryogenic tunnel operation, 100 K	41
10	Loci of energy required for balanced cryogenic tunnel operation, 200 K	42
11	Loci of energy required for balanced cryogenic tunnel operation, 300 K	43
12	Passive bleed boundary-layer control scheme, gas makeup	44
13	Passive bleed boundary-layer control scheme, liquid makeup	45
14	Recirculation mode boundary-layer control	46
15	Partial recirculation mode boundary-layer control	47
16	Makeup of mass flow loci, 100 K	48
17	Makeup of mass flow loci, 200 K	49
18	Makeup of mass flow loci, 300 K	50
19	Spatial profile of tunnel flow Mach number	51
20	Test direction design—least energy consumption locus	52
21	Liquid and gaseous nitrogen management schematic	53
22	Gas bleed capability of tunnel pressure bleed valves at 100 K, M = 0.9	54
23	Gas bleed capability of tunnel pressure bleed valves at 100 K, M = 0.6	55
24	Gas bleed capability of tunnel pressure bleed valves at 300 K, M = 0.9	56
25	Gas bleed capability of tunnel pressure bleed valves at 300 K, M = 0.6	57

EFFECTS OF BOUNDARY-LAYER TREATMENT ON CRYOGENIC WIND-TUNNEL CONTROLS

By

S. Balakrishna*

INTRODUCTION

An important requirement of fluid flow in the test section of a transonic wind tunnel is that true two-dimensional flow field should exist on the model and in its wake for various airfoil profiles and sizes. The control of flow field quality over the model is usually realized by treatment of the side wall boundary layer in the critical regions around the model. The side wall boundary layer is usually treated by removing precise amounts of mass flow of the boundary layer through the porous plates mounted near the model and the slots located just ahead of the model section (ref. 4).

The NASA/LaRC 0.3-meter Transonic Cryogenic Tunnel (0.3-m TCT) is a closed-circuit, fan-driven, liquid nitrogen cooled, gaseous nitrogen medium pressure tunnel capable of full-scale flow Reynolds number and capable of independent control of the tunnel test section flow parameters: Reynolds number Re, test section Mach number M, and flow dynamic pressure q (ref. 5). This unique feature of the cryogenic tunnel is realized by independent control of the three tunnel flow variables: tunnel total pressure P, total temperature T, and test section mass flow $\dot{m}_{ts}$. In turn, independent control of the tunnel flow variables is realized by the three tunnel control inputs: inlet liquid nitrogen mass flow rate $\dot{m}_L$, bleed gas mass flow rate $\dot{m}_g$, and fan speed N. The dynamic model of a cryogenic tunnel has been synthesized, validated, and reported in reference 1. Based on this model, designs of the control laws for closed-loop control of the tunnel pressure P, temperature T, and Mach number M have been generated and successfully realized on the 0.3-m TCT (ref. 2).

---

* Research Associate of Mechanical Engineering and Mechanics, Old Dominion University Research Foundation, P.O. Box 6369, Norfolk, Virginia 23508 (on leave from National Aeronautical Laboratory, Bangalore 560 017, India).

When a cryogenic tunnel operates under steady-state equilibrium conditions, it is a thermodynamic system in which mass-energy control inputs are interactive and are forced to cancel each other. If, in such a cryogenic tunnel, a boundary-layer treatment scheme is incorporated, the basic thermodynamic equilibrium is upset.

In this report, various techniques of realizing the desired boundary-layer wall mass removal are considered so as to obtain the desired flow field over the model for various airfoils. The complementary problem of overall thermodynamic equilibrium maintenance created by the new side wall boundary-layer bleed is considered. This analysis leads to a discussion of the adequacy of the existing tunnel control schemes of reference 2 to accomodate mass-energy disturbances, so that tunnel control is available throughout the desired range of boundary-layer treatment.

NOMENCLATURE

A	test section area, m^2
AB	area of the boundary-layer bleed valves, percent
B	constant associated with compressibility factor
CD	full open flow coefficient of the boundary-layer bleed valve
C_m	specific heat of tunnel metal walls, kJ/kg-K
C_p	specific heat of GN_2 at constant pressure, kJ/kg-K
C_v	specific heat of GN_2 at constant volume, kJ/kg-K
D	constant associated with compressibility factor
E	energy, J
GN_2	gaseous nitrogen
h	enthalpy, kJ/kg
K	constant (or kelvin)
LN_2	liquid nitrogen
M	test section flow Mach number
MB	boundary-layer bleed mass flow, kg/sec
PI	proportional-integral

$\dot{m}$	mass flow rate, kg/sec
N	fan speed, rpm
(1-x)	fraction of mass recirculated $0 < x < 1$
P	tunnel pressure, atm
q	flow dynamic pressure, kg/m^2
Q	heat, J
Re	Reynolds number
T	tunnel gas temperature
W	mass
z	compressibility factor, $z = 1 - P\ e^{D} - P^2\ e^{B}$
y	heat transfer coefficient, J/m^2K-sec
α	cooling capacity of gaseous nitrogen, kJ/kg
β	cooling capacity of liquid nitrogen, kJ/kg
γ	ratio of specific heats
δ	increment
ϵ	fractional flow of test section
σ	asymmetry factor associated with boundary-layer bleed
ξ	percent of test section mass flow, $\xi = 100 \cdot \epsilon$

Subscripts

s	static
L	liquid nitrogen
g	gaseous nitrogen
m	makeup
b	boundary layer
ts	test section
F	fan
Lw	liquid nitrogen flow without boundary-layer bleed

Subscripts (concluded)

Gw gaseous nitrogen flow without boundary-layer bleed

H heater

1,2 valves 1 and 2

CRYOGENIC TUNNEL UNDER EQUILIBRIUM

The schematic diagram of a closed-circuit, fan-driven, cryogenic tunnel cooled by liquid nitrogen sprayed into the tunnel and regulated by gaseous nitrogen bleed is shown in figure 1. The tunnel can be considered a thermodynamically autonomous open system with mass and enthalpy crossing the boundary of the system in the form of fan-induced energy, liquid nitrogen mass flow in with its negative enthalpy, and gaseous nitrogen bleed mass flow out with the negative enthalpy. Assuming that perfect mixing and evaporation of liquid nitrogen into the tunnel resident mass flow occurs, that no work is performed by tunnel gas and that gas behaves perfectly we have

$$\dot{E} = \dot{m}_L h_L - \dot{m}_g h_g + \dot{Q}_F \tag{1}$$

where

$$h_g = C_p T \text{ for perfect gas}$$

and

$$\dot{W}_g = \dot{m}_L - \dot{m}_g \tag{2}$$

Under balanced tunnel conditions, the tunnel $\dot{E}$ and $\dot{W}_g$ tend to zero. The tunnel controls are set up to render the mass and energy rate to zero for finite $\dot{m}_L$ and $\dot{m}_g$. The thermodynamic model of a cryogenic tunnel with a finite metal mass is shown in figure 2. The effect of metal mass is relevant only under dynamic temperature conditions; hence, its effect is ignored in the bulk of this analysis.

The mass energy interaction associated with the cryogenic tunnel resident gas mass and the control inputs can be graphically analyzed using the energy state diagram (ref. 1). The energy state diagram of the gas resident in a vessel is the plot of its mass and internal energy for various gaseous states (fig. 3). The loci of constant temperature are lines of slope C_vT radiating from the origin, and the loci of constant pressure are lines running generally parallel to the mass axis. Given a specific state of gas defined by point A in figure 3, the introduction of mass and energy rate control vectors can be graphically represented by three mass-energy rate vectors: $(\dot{m}_L, \dot{m}_L h_L)$, $(-\dot{m}_g, -\dot{m}_g C_p T)$, and $(0, \dot{Q}_F)$. The net sum of these mass-energy vectors provides the final state of tunnel gas. Under equilibrium conditions, the control vectors cancel each other as described by equations (1) and (2).

Any scheme which provides for aspiration of the boundary layer upsets the mass equilibrium of equation (2). In the following sections, various schemes for removal of boundary-layer mass flow and extra controls needed to maintain thermodynamic equilibrium are analyzed.

BOUNDARY-LAYER TREATMENT SCHEMES

The flow field over a model in the test section of a wind tunnel at transonic speeds is particularly sensitive to the side wall boundary-layer growth and the airfoil geometry. In the 0.3-m TCT facility, it is proposed to control the side wall boundary-layer around the model by removing a certain amount of mass flow through the porous plates around the model and/or the slotted side walls. This two-zone mass removal is expected to provide adequate control in realizing the desired two-dimensional flow field over the model. The schematic diagram of figure 4 details the plans for symmetrical removal of mass flow from the two side walls through two ducts on each side. The magnitude of the mass flow removed from the side walls is based on the magnitude of the test section mass flow. Typically

$\dot{m}_b$ = total side wall boundary-layer bleed

$= \varepsilon \cdot \dot{m}_{ts}$

where ϵ is the fraction of the test section flow with $0 < \epsilon < 0.04$, and $\dot{m}_{ts}$ is the test section mass flow.

The test section mass flow in a transonic tunnel is

$$\dot{m}_{ts} = 6965\ A \frac{PM}{\sqrt{T}} (1 + 0.2\ M^2)^{-3}\ \text{kg/sec} \tag{3}$$

Hence

$$\dot{m}_b = \epsilon\ \dot{m}_{ts} = 6965 \frac{PMA}{\sqrt{T}} (1 + 0.2\ M^2)^{-3}\ \epsilon \tag{4}$$

or

$$\frac{\dot{m}_b}{P} = 6965 \frac{MA\epsilon}{\sqrt{T}} (1 + 0.2\ M^2)^{-3}\ \text{kg/sec/atm} \tag{5}$$

The side wall boundary-layer pressure is the local static pressure described by the isentropic expression

$$P_s = P(1 + 0.2\ M^2)^{-3.5} \tag{6}$$

Though the local temperature at side wall is the static temperature, the moment gas stagnates the temperature recovery is likely to recover to its total value T.

In order to realize good flow-field control, $\dot{m}_b$ is to be removed from the tunnel side wall. A plot of the boundary-layer bleed mass flow $\dot{m}_b/P$ is shown in figure 5 as a function of flow Mach number M. The 8 loci of figure 5 correspond to ϵ = 0.005 to 0.04, in steps of 0.005, for a tunnel gas temperature of 100 K. Typically the mass flow $\dot{m}_b/P$ ranges up to about 2 kg/sec/atm. Figures 6 and 7 provide corresponding $\dot{m}_b/P$ loci for various Mach numbers and percentile bleed flows at 200 K and 300 K. Figure 8 illustrates the minimum total pressure at which passive bleed to atmosphere can be realized based on equation 6.

BOUNDARY-LAYER BLEED MASS FLOW MANAGEMENT

Consider a cryogenic, transonic, wind tunnel operating at tunnel total pressure of P, total temperature T, and a test section mass flow M. The tunnel fan induces gas motion around the tunnel and, in turn, $\dot{Q}_F$ where

$$\dot{Q}_F = \frac{K_F\ P\sqrt{T}\ M^3}{(1 + 0.2\ M^2)^3}\ \text{kJ/sec} \tag{7}$$

If a mass flow of $\dot{m}_b$ is removed from the side walls and discharged to atmosphere, the tunnel thermodynamic balance is upset with the new tunnel energy mass states as

$$\dot{E} = \dot{Q}_F - \dot{m}_b h_b = \dot{Q}_F - \dot{m}_b C_p T \tag{8}$$

$$\dot{W}_g = -\dot{m}_b \tag{9}$$

If the tunnel pressure and temperature are to be regulated, mass energy control inputs are necessary to render $\dot{E}$ and $\dot{W}_g$ to zero.

The plots of normalized mass flow inputs necessary for tunnel balance, $\dot{m}_b/P$, are shown in figures 5, 6, and 7 for 3 representative tunnel gas temperatures of 100, 200, and 300 K. The mass flow magnitudes range up to 2 kg/sec/atm at their maximum. The energy input necessary for tunnel energy balance is $-\dot{E}/P$. The plots of energy needed for tunnel balance, $-(\dot{Q}_F - \dot{m}_b C_p T)/P$, are shown in figures 9, 10, and 11. Figure 9, corresponding to a gas temperature of 100 K, illustrates 8 loci of $-\dot{E}/P$ for various side wall boundary-layer mass flow factors ϵ ranging from 0.005 to 0.04 in steps of 0.005 as a function of tunnel test section flow Mach number M. The energy needed for tunnel balance takes on bipolar values. At very low Mach numbers, positive energy is needed for tunnel balance. With increasing Mach number, the energy needed increases and peaks between 0.4 and 0.55. Subsequently, the energy needed for tunnel balance drops off and tends to negative values. Figures 10 and 11 indicate new energy required for tunnel balance of gas temperatures of 200 and 300 K,

respectively. Hence, figures 5 to 7 provide the mass required for tunnel mass balance, and figures 9 to 11 provide energy required for tunnel energy balance in order to provide adequate boundary-layer treatment bleed mass flow and yet maintain the tunnel thermodynamic equilibrium.

Two basic schemes of mass and energy management are now considered and analyzed. In the first scheme, the boundary-layer treatment mass flow is passively discharged to atmosphere. The resulting mass-enthalpy imbalance is made up from external sources. Two methods of mass-energy are considered: In the first method, the mass makeup is from a gaseous nitrogen source which possesses adequate enthalpy and is illustrated in figure 12. In the second method, the mass shortfall is made up from the liquid nitrogen source and the energy shortfall is made up by introducing a heater in the tunnel. This method is illustrated in figure 13.

In the second scheme of mass and energy management, the boundary-layer treatment mass flow is either partially or fully reinjected and recirculated. Figure 14 illustrates a scheme for recirculation of the full mass flow treated out of the boundary layer. Figure 15 illustrates a scheme for partial mass flow recirculation with the rest discharged to atmosphere. In the following analysis, these four methods of boundary-layer treatment are detailed.

PASSIVE BOUNDARY-LAYER BLEED CONTROL

Introduction

Consider the thermodynamic system of figure 12 corresponding to the 0.3-m TCT operating at pressure P, temperature T, Mach number M, and boundary-layer bleed mass flow $\dot{m}_b$. If there were no boundary-layer bleed mass flow $\dot{m}_b$, the cryogenic tunnel would have a mass energy control law described by

$$\dot{m}_{Lw} = \dot{m}_{Gw} = - \frac{\dot{Q}_F}{h_L - C_p T} \tag{10}$$

This is realized by regulating $\dot{m}_{Lw}$ to achieve constant temperature and $\dot{m}_{Gw}$ to achieve constant pressure as described in reference 2.

If the boundary-layer mass flow control valve is now opened to atmosphere such that a precise amount $\dot{m}_b = \varepsilon \dot{m}_{ts}$ is discharged, the desired flow field control can be had. However, the mass balance of the tunnel is upset. In order to create passive mass flow out of the tunnel test section to atmosphere, the tunnel static pressure P_s should be at least 1 atm. This can be assured only when the tunnel total pressure is $(1 + 0.2\ M^2)^{3.5}$ atm. Figure 8 illustrates the minimum tunnel total pressure essential for the passive bleed mode of the boundary-layer mass flow control. The cryogenic tunnel mass balance is dominantly controlled by the magnitude of difference flow $\dot{m}_b - \dot{m}_{Lw}$. The properties of this difference flow are now analyzed:

$$\frac{\dot{m}_b - \dot{m}_{Lw}}{P} = \frac{\varepsilon \dot{m}_{ts} - \dot{m}_{Lw}}{P} = \frac{6965\ \varepsilon A}{\sqrt{T}} M(1 + 0.2\ M^2)^{-3}$$

$$- \frac{K_F \sqrt{T}\ M^3}{h_L - C_p T} (1 + 0.2\ M^2)^{-3} \qquad (11)$$

This difference mass flow normalized to tunnel total pressure is plotted as a function of Mach number $0.2 \leq M \leq 1$ and boundary-layer bleed mass flow fractional factor $0 \leq \varepsilon < 0.04$, in steps of 0.005 at different tunnel temperatures.

Figure 16 illustrates the difference mass flow $\frac{\dot{m}_b - \dot{m}_{Lw}}{P}$ for tunnel gas temperature of 100 K. Eight loci on figure 16 correspond to a boundary-layer bleed mass flow of 0.5 to 4 percent of test section flow. At low Mach numbers near 0.2, the difference flow is positive, indicating a need for extra makeup mass flow $\dot{m}_m = \dot{m}_b - \dot{m}_{Lw}$. The makeup mass flow $\dot{m}_m$ increases with Mach number and peaks at a value of M varying from 0.4 to 0.55. For higher Mach numbers the difference mass flow drops. At low values of ε, the difference swings over to negative values at Mach 1, and at higher values of ε the difference stays positive even at M = 1, as illustrated in figure 16. Typically, a maximum makeup mass flow of 1 kg/sec/atm is needed at peak demand.

Similarly, figures 17 and 18 illustrate the loci of difference flow corresponding to gas temperatures of 200 and 300 K. These loci show properties similar to the 100 K case except that the magnitude of $\dot{m}_m$ drops off because of higher effectiveness of liquid nitrogen in cooling.

When the boundary-layer bleed mass flow $\dot{m}_b < \dot{m}_{Lw}$, corresponding to the case of tunnel operation lower than zero line in figures 16, 17, and 18, the tunnel temperature and pressure control schemes discussed in reference 2 can adequately regulate the tunnel conditions as described by

$$\left.\begin{aligned} \dot{E} = 0 &= \dot{Q}_F + \dot{m}_{Lw} h_L - (\dot{m}_g + \dot{m}_b) C_p T \\ \dot{W}_g &= 0;\ \dot{m}_g + \dot{m}_b = \dot{m}_{Lw} = \dot{m}_{Gw} \end{aligned}\right\} \qquad (12)$$

The temperature control loop function is not affected. However, the pressure control loop adapts to the boundary-layer bleed by reducing the big end flow from $\dot{m}_{Gw}$ to $\dot{m}_g$ such that $\dot{m}_b + \dot{m}_g = \dot{m}_{Gw} = \dot{m}_{Lw}$. The bled-off boundary-layer mass flow acts as a mass flow disturbance to the pressure loop. The pressure loop accomodates this disturbance without any error since the pressure loop is type 1 (ref. 2).

Gas Makeup

When the boundary-layer bleed mass flow $\dot{m}_b > \dot{m}_{Lw}$, corresponding to operating the tunnel above the zero line in figures 16, 17, and 18, a new strategy (illustrated in figure 11) is essential for tunnel thermodynamic mass-energy balance. Since the outgoing mass flow $\dot{m}_b$ is larger than incoming flow $\dot{m}_{Lw}$, new makeup mass flow $\dot{m}_m$ is necessary for mass equilibrium. Further, to maintain energy balance, makeup mass flow $\dot{m}_m$ should have an enthalpy h_m. The thermodynamic balance is to be realized as in equations

$$\left.\begin{aligned} \dot{E} = 0 &= \dot{Q}_F + \dot{m}_L h_L - \dot{m}_b C_p T + \dot{m}_m h_m \\ \dot{W}_g &= 0;\ \dot{m}_m = \dot{m}_b - \dot{m}_{Lw} \end{aligned}\right\} \qquad (13)$$

Since the fan heat is $\dot{Q}_F = -\dot{m}_{Lw} (h_L - C_p T)$, equation (13) can be simplified to arrive at h_m necessary to maintain energy balance:

$$h_m = \frac{-\dot{Q}_F - \dot{m}_{Lw} C_p T + \dot{m}_{Lw} h_L + \dot{m}_m C_p T}{\dot{m}_m} = \frac{\dot{m}_m C_p T}{\dot{m}_m} = C_p T \qquad (14)$$

Thus a mass flow $\dot{m}_m$ at a positive enthalpy $h_m = C_p T$ is necessary to maintain tunnel conditions, which indicates that the source of makeup could be a gas reservoir storing gas at the same temperature as the tunnel. This has been illustrated in figure 12. The gas reservoir feeds the tunnel at a rate of $\dot{m}_m$ at an enthalpy of $C_p T$, and the tunnel controls generate $\dot{m}_{Lw}$ liquid nitrogen flow. When the boundary-layer valves are opened to create $\dot{m}_b$, the pressure control valve moves $\dot{m}_g$ to zero.

If the gas enthalpy is less than $C_p T$, the temperature or energy balance is not assured. However, if the gas has an enthalpy greater than $C_p T$, tunnel controls will work as discussed below. Let the incoming mass flow be $\dot{m}_m + \Delta\dot{m}_m$ at an enthalpy $C_p T + \Delta h_m$. The control law discussed in reference 2 will force an extra amount of liquid $\Delta\dot{m}_L$ to cancel the extra enthalpy, and the pressure loop will discharge the extra mass $\Delta\dot{m}_L + \Delta\dot{m}_m$ as $\dot{m}_g$. This thermodynamic equilibrium can be represented as

$$\left.\begin{aligned} \dot{W}_g &= 0 = \dot{m}_m + \dot{m}_{Lw} - \dot{m}_b - \dot{m}_g + \Delta\dot{m}_L + \Delta\dot{m}_m ; \; \dot{m}_g = \Delta\dot{m}_L + \Delta\dot{m}_m \\ \dot{E} &= 0 = \dot{Q}_F + (\dot{m}_{Lw} + \Delta\dot{m}_L)\, h_L - \dot{m}_b C_p T - \dot{m}_g C_p T \\ &\quad + (\dot{m}_m + \Delta\dot{m}_m)\,(C_p T + \Delta h_m) \end{aligned}\right\}$$

simplifying $\dot{E} = 0$, we have

$$\Delta\dot{m}_L = \dot{m}_m \frac{\Delta h_m}{h_L - C_p T} \text{ (ignoring enthalpy } \Delta\dot{m}_m \Delta h_m) \qquad (15)$$

In summary, a cryogenic wind tunnel, which operates with temperature and pressure control laws described in reference 2, can accomodate boundary-layer passive bleed treatment to its test section flow field. As long as $\dot{m}_b < \dot{m}_{Lw}$, no extra facilities are required. However, when $\dot{m}_b = \epsilon\dot{m}_{ts} > \dot{m}_{Lw}$, a gaseous mass flow $\dot{m}_m \geq \dot{m}_b - \dot{m}_{Lw}$ should be passively dumped into the tunnel and its temperature must be greater than tunnel temperature T. This makeup mass flow does not require any active closed-loop controls as long as $\dot{m}_m > \dot{m}_b - \dot{m}_{Lw}$ and $h_m > C_p T$. Under these conditions, the active closed-loop

controls accomodate the new mass entry and boundary-layer bleed and still maintain tunnel pressure and temperature.

Liquid Nitrogen Makeup

In a cryogenic tunnel, a passive discharge boundary-layer treatment dictates an addition of new mass and enthalpy into the tunnel, as detailed in the previous section. The mass requirement $\dot{m}_m$, shown in figures 16 to 18, is needed only when $\dot{m}_m = \dot{m}_b - \dot{m}_{Lw} > 0$, and it should possess an enthalpy of $h_m \geq C_p T$.

If the makeup mass flow $\dot{m}_m$, when greater than zero, were to be from a liquid nitrogen source, then the enthalpy associated with the makeup mass would be h_L, which is negative. This would upset the energy balance. However, if adequate heat is added into the system such that $\dot{Q}_H \geq -h_L + C_p T$, then mass and energy balance conditions can exist.

Consider the thermodynamic schematic diagram in figure 13. This shows a cryogenic tunnel at conditions P, T, and M, generating fan-induced heat $\dot{Q}_F$. Let an electrical heater of capacity greater than $\dot{Q}_H$ be added. If from this tunnel a mass flow $\dot{m}_b = \varepsilon \dot{m}_{ts}$ is removed such that $\dot{m}_m = \dot{m}_b - \dot{m}_{Lw} > 0$, then the following thermodynamic balance can exist. Firstly, the automatic temperature control system opposes the heat $\dot{Q}_F + \dot{Q}_H$, and hence generates a mass flow $\dot{m}_{Lw} + \dot{m}_m$; the pressure loop control law enforces the mass balance as long as $\dot{m}_g > 0$, but tends to zero. Hence

$$\dot{m}_b = \varepsilon \dot{m}_{ts} > \dot{m}_{Lw}$$

$$\dot{E} = 0 = \dot{Q}_F + \dot{Q}_H + (\dot{m}_{Lw} + \dot{m}_m)\, h_L - (\dot{m}_b + \overset{\to 0}{\dot{m}_g}) C_p T$$

$$\dot{W}_g = 0;\ \dot{m}_m + \dot{m}_{Lw} = \dot{m}_b + \overset{\to 0}{\dot{m}_g}$$

Further

$$\dot{m}_{Lw} = \frac{-\dot{Q}_F}{h_L - C_p T};\quad \dot{m}_m = \frac{-\dot{Q}_H}{h_L - C_p T} \tag{16}$$

The minimum heater capacity is estimated on the basis of $\dot{Q}_H = -\dot{m}_m \cdot (h_L - C_p T)$ and can be found directly from figures 16 to 18. At a gas temperature of 100 K and at a tunnel pressure of 6 atm, the maximum heater energy rate occurs at about M = 0.55 and corresponds to 1590 kW. Similarly, peak heater capacities of 1560 kW and 1515 kW can be estimated for T = 200 K and T = 300 K, respectively.

In order to realize adequate boundary-layer bleed flow, $\dot{Q}_H$ is estimated from figures 16 to 18 or from equations (11) and (16).

Initially the tunnel is run up to conditions P, T, and M without boundary-layer bleed on automatic temperature and pressure controls. Then the heater is switched on to generate $\dot{Q}_H$, simultaneously passively opening boundary-layer valves to realize $\dot{m}_b$. The temperature loop sensing extra heat pumps in $\dot{m}_{Lw} + \dot{m}_m$ amount of liquid nitrogen and the boundary-layer valve discharges $\dot{m}_b$. The big end pressure valve works near zero, but at a positive mass flow, and regulates the tunnel pressure. To keep $\dot{m}_g$ positive, a heat in excess of $\dot{Q}_H$ is generated. In this scheme, no automatic controls are necessary. The other major advantage of this scheme is that no gas tank, gas valves, or ducts are required. Further, a need for maintaining gas tank pressure in excess of tunnel pressure does not arise.

It may be noted that, in both the passive boundary-layer bleed schemes, the makeup mass flow $\dot{m}_m$ is derived from the nitrogen tank. In the case of gas makeup, the mass flow $\dot{m}_m$ initially evaporates into the gas tank and is used as makeup mass flow. In the case of liquid nitrogen makeup, the mass flow $\dot{m}_m$ is directly derived from the LN_2 source. Thus, the nitrogen consumption in either case is the same. The energy for evaporating the liquid nitrogen mass $\dot{m}_m$ is derived from the ambient in the case of the gas makeup scheme. After building up pressure in excess of tunnel pressure, the gas flow valve can be used to create necessary flow. In the case of liquid nitrogen makeup, the energy for evaporating liquid mass $\dot{m}_m$ is derived from the electrical heater.

The disadvantages of the gas makeup scheme are that a gas tank of adequate volume is necessary, together with a flow control valve, nonreturn valve, and associated plumbing. The system does not work unless adequate

gas pressure and temperature exist. The mass flow control is involved because of depleting pressure in the gas tank unless the evaporator is able to handle the full mass flow rate.

In the case of LN_2 makeup with heater, no gas handling equipment is necessary. A heater of adequate capacity and smooth control is essential. Further, extra energy is required to evaporate liquid mass $\dot{m}_m$.

In summary, the addition of a heater capable of generating heat forces the temperature control system to increase liquid nitrogen flow such that $\dot{m}_{Lw} + \dot{m}_m \geq \dot{m}_b$. The heater control can be open loop, and no other controls are required to realize the necessary passive bleed of boundary layer to atmosphere.

RECIRCULATION MODE BOUNDARY-LAYER CONTROL

Another solution to the problem of maintaining mass-energy balance in a cryogenic tunnel, while removing $\dot{m}_b = \epsilon\dot{m}_{ts}$ through the side walls of the test section boundary layer, is to either partially or totally reinject this mass into the tunnel elsewhere.

A scheme for total reinjection of the boundary-layer treatment mass flow $\dot{m}_b$ is illustrated in figure 14. In this scheme, the boundary-layer bleed mass flow $\dot{m}_b$ is inducted fully by a recirculation fan/compressor and is reinjected in the liquid nitrogen injection section. Obviously by this treatment the mass balance of the tunnel is not upset. However, in creating the necessary pressure ratio across the fan, work is done on $\dot{m}_b$, resulting in dissipation of heat $\dot{Q}_b$ into the gas. A new thermodynamic balance now needs to exist which allows cooling of this extra heat $\dot{Q}_b$ by injecting an extra liquid nitrogen mass $\dot{m}_{Lb}$ and discharging it through the pressure control valve. The new thermodynamic balance can be expressed as

$$\dot{Q}_b = \dot{m}_b C_p \delta T$$

where δT is the temperature rise across the recirculation fan/compressor.

$$\left.\begin{aligned} \dot{E} = 0 &= \dot{Q}_F + \dot{Q}_b + (\dot{m}_{Lw} + \dot{m}_{Lb})\, h_L - \dot{m}_g C_p T \\ \dot{W}_g &= 0;\ \dot{m}_g = \dot{m}_{Lw} + \dot{m}_{Lb} = -\left(\frac{\dot{Q}_F + \dot{Q}_b}{h_L - C_p T}\right) \\ \dot{m}_{Lb} &= \frac{-\dot{Q}_b}{h_L - C_p T} \end{aligned}\right\} \qquad (17)$$

Even in this scheme, as long as $\dot{m}_b < \dot{m}_{Lw}$, active recirculation can be avoided by passive discharge of $\dot{m}_b$ to the atmosphere. However, once $\dot{m}_b$ exceeds $\dot{m}_{Lw}$, the recirculation fan can be operated. In this scheme, extra energy is consumed in the form of $\dot{Q}_b$ and $\dot{m}_{Lb}$. Further, the choice of a fan which can efficiently handle mass flow $\dot{m}_b$ which varies from 0 to 0.04 $\dot{m}_{ts}$ is likely to be formidable because of the surge behavior of most fans, particularly at low mass flows. Figures 5 to 7 provide an idea of the mass flow needed for recirculation of boundary-layer bleed mass flow.

Another solution to boundary-layer treatment mass management is to partially recirculate the mass flow $\dot{m}_b$. In this scheme, illustrated in figure 15, the big end flow $\dot{m}_g$ is kept quiescently near zero. Only a part of the boundary-layer bleed $\dot{m}_b$ is recirculated, thereby reducing heat $\dot{Q}_b$ and, hence, the need for large values of $\dot{m}_{Lb}$:

$$\left.\begin{aligned} & x < 1;\ \dot{m}_b > \dot{m}_{Lw} \\ & x\,\dot{m}_b = \dot{m}_{Lw} + \dot{m}_{Lb};\ \dot{m}_b = \epsilon \dot{m}_{ts} \\ & \dot{m}_{Lw} + \dot{m}_{Lb} = \frac{-\left(\dot{Q}_F + \dot{Q}_b\right)}{h_L - C_p T};\ \dot{m}_{Lb} = \frac{-\dot{Q}_b}{h_L - C_p T} \\ \text{and} \quad & \dot{Q}_b = (1 - x)\,\dot{m}_b\, C_p\, \delta T \end{aligned}\right\} \qquad (18)$$

In this scheme, heat $\dot{Q}_b$, δT, and $\dot{m}_{Lb}$ are likely to be smaller than they would be with full reinjection of boundary-layer mass.

As regards the controls necessary for the recirculation scheme, the basic tunnel temperature and pressure controls can maintain tunnel conditions as long as the recirculation fan is able to function steadily. Due to varying $\dot{m}_b$ requirements, the ability of the recirculation compressor to precisely regulate the mass flow $\dot{m}_b$ makes compressor design complex. The need for both speed control and throttle control with backup, to assure operation below surge line, exists. In the partial reinjection scheme, in addition to fan/compressor mass flow controls, automatic area adjustments to the atmosphere bleed line may be necessary.

In comparing the four schemes for boundary-layer management, the scheme of passive bleed with liquid nitrogen makeup and a heater appears to be most simple from the control point of view. However, this scheme requires design of an electrical heater and consumes considerable power. It does not require any gas handling schemes either in the form of a compressor or gas tank. This scheme is the least energy efficient, but is the simplest.

The recirculation schemes are energy efficient, but the controls for these schemes are very complex. The need for compressor antisurge-mass flow controls exists and may truncate the performance range at very low mass flows.

The gas makeup scheme is a little more energy efficient than the liquid makeup scheme with heater. However, the gas makeup scheme requires extra controls to maintain mass flow rates and considerable gas evaporation equipment.

ENGINEERING CONSIDERATIONS FOR VARIOUS BOUNDARY-LAYER TREATMENT SCHEMES

Heater Design

Introduction of an electrical heater into the tunnel stream has been found to generate more liquid nitrogen flow into a cryogenic tunnel which can then be discharged as warmer tunnel gas through the boundary-layer treatment valves. Since the excess liquid or gas mass is directly related to the amount of heat-induced $\dot{Q}_H$, an electrical heater whose power is controllable directly controls $\dot{Q}_H$ and $\dot{m}_b$ as discussed in previous sections.

In a cryogenic tunnel, the operating gas temperature ranges from about 80 to 300 K. Any electrical heater required to operate in such a medium should possess adequate resistivity to generate necessary heat. The temperature coefficient of resistance is the parameter which describes resistivity of the heater material, and in a cryogenic environment the temperature coefficient of resistance must be near zero with the resistivity itself being large.

A study of electrical properties of some special alloys indicates that constantan (an alloy of 60 percent copper and 40 percent nickel) and marganin (an alloy of 84 percent copper, 12 percent manganese, and 4 percent nickel) have very low temperature coefficients. Typically these are two to five parts per million of the resistance. Hence, over the temperature range of 80 K to 300 K, the resistance charge is 2 to 4 percent.

Manganin is a traditionally used, high-stability, resistance material. Design of a heater capable of 1600 kW dissipation is now considered and matched to the 0.3-m cryogenic tunnel. Figure 19 indicates the flow local Mach number profile in the 0.3-m TCT. The heater location should preferably be in a high-speed flow area, but its presence should not create excessive tunnel blockage. In the present analysis, location of the heater downstream of fan nacelle is considered. The local Mach number of flow is 0.18 when the test section Mach number is 0.55, at which peak power demand occurs. It is at this operating point the heater design is evaluated. The heat transfer from the heater to gas stream is dominantly by forced convection heat transfer.

The heater coil design for 1600 kW can be based on a voltage of 1000 V at 1600 amperes. To carry 1600 amperes, a manganin wire of 1.13-cm diameter, corresponding to 1 cm^2 area, is used. A resistance of 0.667 ohms is desired. The resistivity of manganin is 44×10^{-4} ohm cm, and hence a 150-m length of wire is desired. This wire has a surface area of 5.32 m^2. The wire could be disposed in a 60-cm coil of 78 loops located downstream of the fan nacelle.

The heat transfer coefficient for forced convection, from reference 1, is

$$y = 8.234\ P^{0.8}\ T^{-0.22}\ M(1 - 0.67\ M^{0.65})\ kJ/m^2/K/sec \qquad (19)$$

Based on this coefficient, the maximum temperature rise design can be made.

In reference 3, the minimum energy test direction design has been detailed. A major conclusion of that report is that the tunnel operation locus is a minimum pressure, minimum temperature line of figure 20. Thus, at 300 K operation, the tunnel pressure need not exceed 1.2 atm. Under such a condition, the heater temperature rise can be estimated: $\dot{Q}_H$ (from figure 18) at 1.2 atm is 320 kW. To dissipate 320 kW, the temperature rise is estimated on a basis of P = 1.2 atm, T = 300 K, and $M_{local} = 0.18$:

$$\delta T = \frac{\dot{Q}_H}{y} = 161\ K$$

Hence the heater element is likely to work at 461 K at tunnel conditions of P = 1.2 atm, T = 300 K, M = 0.55, and $M_{local} = 0.18$, while to create $\dot{m}_b = 0.04\ \dot{m}_{ts}$ a heat of 320 kW is required.

At the other extreme of M = 0.55, P = 6 atm, and T = 100 K, a similar temperature rise estimate can be made. From figure 16, $\dot{Q}_H$ can be estimated as 1590 kW. Hence

$$\delta T = \frac{\dot{Q}_H}{y} = 223\ K$$

The heater element is likely to work at 323 K when the tunnel operates at 100 K, M = 0.55, and P = 6 with a 4 percent boundary-layer bleed.

When the heater elements work at such temperatures, radiation of heat to wall can be a problem since the symmetrically placed element coil is typically 10 cm away from wall (80-cm duct diameter accommodates a 60-cm coil). Appropriate thermal analysis of that segment needs to be performed.

The proposed heater is a 0.667 ohm, 1.13-cm diameter, 150-m long manganin coil of 60-cm outside diameter and 59-cm mean diameter disposed in

about 80 coils. The gap between coils is about 2 cm, making the heater about 2.4-m long. The heater is to be supported by cryogenic compatible supports in the 80-cm inside diameter duct. The heater wires are to enter the tunnel through two pressure seal connectors.

The electrical control system needed to generate the heat is a simple 2 MVA transformer of 1000 V, 60 Hz AC, which can be used in a simple, auto-transformer mode providing 0 to 1000 VAC. A thyristor-based cyclo switching system can also be used to avoid the brush problems of an autotransformer. Adequate interlocks are to be planned to provide heating only when the tunnel flow is on, so as to ensure convection heat transfer. Backup interlocks in the form of tunnel wall temperature or heater element temperature can also be included.

It may be noted that the heater and its support are likely to introduce 4 to 5 percent blockage in the return leg and will have their secondary effects on tunnel fan energy consumption and on the tunnel circuit loss factor.

Flow Chart for Passive Boundary-Layer Bleed Schemes

When the boundary-layer treatment is through passive discharge, the mass flow control is realized by valve area control. In figure 4, the two symmetrical valves of area AB_1 and AB_2 perform the bleed operation. In the case of the 0.3-m TCT, 2 digital valves of 11-bit resolution have been chosen. These are linear area control valves compatible for microprocessor-based operation. The mass flow through any valve is

$$\dot{m}_{b1} = \frac{0.6992\ P_s}{\sqrt{TZ}}\ C_D\ AB_1\ \sigma_1 \qquad (20)$$

where P_s is the tunnel test section static pressure in atm;

C_D is the full area valve flow coefficient, $C_D = 3.70$;

AB_1 is the valve area in percent;

σ_1 is the asymmetry factor for fine-tuning mass flow, $0.9 \leq \sigma \leq 1.1$;

T is the tunnel temperature; and

z is the gas compressibility.

For real nitrogen gas (ref. 5),

$$z = 1 - P \exp(D) - P^2 \exp(B) \tag{21}$$

where

$$D = 1.37 - 8.77\ T \times 10^{-2} + 4.7\ T^2 \times 10^{-4} - 1.38\ T^3 \times 10^{-6} + 1.46\ T^4 \times 10^{-9}$$

and

$$B = 5.52 - 1.98\ T \times 10^{-1} + 7.81\ T^2 \times 10^{-4} - 1.26\ T^3 \times 10^{-6} + 5.3\ T^4 \times 10^{-10}$$

Hence, by controlling the valve areas AB_1 and AB_2, the control of mass flow MB1 + MB2 = $\dot{m}_b$ can be had.

A flow chart for designing a microprocessor-based controller to control the two digital valves is shown in the appendix. This flow chart accommodates four modes of operation: Manual, Hold, Auto 1, and Auto 2.

In the Manual mode, the valve area is controlled by thumbwheel input controls for each valve. Since the valve has 11-bit resolution, the input control can have a 3 to 4 digit command capability. The provision has been made for automatically reading the desired valve areas AB_1 and AB_2 once every second. The respective mass flows MB_1 and MB_2 are estimated using the valve area, tunnel states, known values of asymmetry coefficients, and the respective mass flows are displayed.

In the Hold mode, the valve areas remain fixed at values of valve area prior to going on Hold mode. However, for fluctuating P and T the mass flow estimations are made every second and displayed.

In the Auto 1 mode, the desired mass flow rates MB_1 and MB_2 are read in from thumbwheel switches in kg/sec. The valve area required for each valve is estimated based on current tunnel pressure and temperature. For varying tunnel P and T, the valve area tracks and provides the

desired flow rate. The estimated valve areas are used to command the digital valve, which has a resolution of 1 in 2000.

In the Auto 2 mode, the thumbwheel inputs provide the desired percentile mass flow ϵ as ϵ_1 and ϵ_2. From these values, the mass flow rates MB_1 and MB_2 are estimated. Subsequently, the mode of operation is similar to Auto 1.

Thus the flow chart in the Appendix provides the basis on which boundary-layer bleed mass flow can be estimated and realized. For this the digital valve calibration is essential. The valve area controls automatically track the tunnel condition variations in the Auto 1 and Auto 2 modes. The rate of update proposed is 1/sec. The disturbances occur once a second, thereby allowing the tunnel pressure and temperature controls, which are faster, to stabilize.

Recirculation Compressor/Fan Performance

The design of the recirculation compressor/fan configurations, illustrated in figures 14 and 15, needed for either total or partial reinjection of the boundary-layer bleed mass flow can be based on mass flow magnitudes $\dot{m}_b$ of figures 5, 6, and 7. The compressor/fan is required to (1) induce a mass flow of $\dot{m}_b$ from the test section side wall valves of figure 4 and (2) create a controlled pressure ratio to account for the suction line pressure losses, discharge duct pressure losses, and the tunnel circuit losses in static pressure between the tunnel test section side walls and the gas reinjection point in the high-speed diffuser. The tunnel circuit losses between these two points can be noted to be a major part of the total tunnel losses. Once the recirculation duct size and configuration is decided, the mass flow-pressure ratio required for fan design is fully known. This desired fan map is a function of M, ϵ, and P.

Without going into detailed quantitative estimations of this desired fan map, it is obvious that for low ϵ and M, the mass flow-pressure combination is likely to take any compressor into the surge zone in a rotary compressor. Appropriate measures are necessary to counter this.

While designing the recirculation fan, the findings of reference 3, which translates given R_e-M to P-T, can be noted. Figure 20, which summarizes test direction design, indicates that tunnel pressure need not be more than 1.2 atm for temperatures of gas other than about 100 K. Thus, while translating figures 5, 6, and 7, tunnel pressures of 5 to 6 atm need be considered only for figure 5.

Tunnel Control Valve Capacities

In absence of any boundary-layer treatment, the basic tunnel control is achieved by manipulating the liquid nitrogen valve area, gas bleed valve area, and fan speed by appropriate closed-loop control laws designed and detailed in reference 2. Figure 21 indicates the schematic of tunnel nitrogen mass management and shows a digital liquid nitrogen control valve which regulates the liquid flow from a liquid nitrogen pump. This system also has a pressure control relief valve. Figure 21 also shows three gas discharge valves, one a fast pressure control valve and the other two slow acting bias flow valves.

As discussed in previous sections, the closed-loop control laws of reference 2 can accommodate boundary-layer treatment schemes whether active recirculation or passive bleed types. In the case of passive bleed, wherein $\dot{m}_b > \dot{m}_{Lw}$, the need for makeup mass flow in excess of $\dot{m}_m$ and enthalpy in excess of h_m assures the satisfactory operation of the controls. In the case of active recirculation, the existing controls are adequate as long as $\dot{m}_{Lb}$, the extra flow, does not exceed the capacity of the liquid nitrogen pump. In the case of the liquid makeup scheme for passive bleed, the maximum liquid nitrogen is consumed when M = 0.55, ϵ = 0.04, P = 6, and T = 100 K, and it corresponds to about 10.7 kg/sec. The liquid pump has a capacity of 15 kg/sec, and hence can accommodate all the boundary-layer schemes of figures 12 to 15.

When gas makeup is used, the makeup gas is derived from a tank with gas at a temperature higher than tunnel gas. Its volume capacity is dictated by the length of the tunnel run. If the tank volume is relatively low, then the valve connecting the tank to the tunnel should be a closed-loop control valve which maintains the incoming mass flow despite varying

tank pressures. This control law is a simple mass flow control of the PI type. A nonreturn valve is necessary to prevent back flow.

When the recirculation mode of boundary-layer control is used, the mass flow out of the big end goes up. At low pressures this could be critical because of unchoked flow. Figures 22 to 26 indicate the bleed mass flow capability of the big end valves of the 0.3-m TCT. At M = 0.9 and 100 K, the control valve by itself cannot handle even the tunnel flow $\dot{m}_{Lw.}$ Hence the bias valves are to be opened. With both the bias valves full open, the system can handle 15 kg/sec at about 3 atm. Figure 22 illustrates the $\dot{m}_g$ capability at 100 K and M = 0.9. Similarly, figures 23 to 25 illustrate the mass discharge capability of the 0.3-m TCT for 100 K and M = 0.6, 300 K and M = 0.9, and 300 K and M = 0.6, respectively.

In summary, the existing valve sizes of the tunnel control systems are sufficient to accommodate any of the four schemes of boundary-layer control discussed.

SUMMARY AND CONCLUDING REMARKS

In order to maintain a uniform, two-dimensional, flow field in the test section of a transonic tunnel, one of the techniques usually used is to aspirate boundary-layer mass flow across the slotted/porous walls of the test section. Typically this mass flow ranges up to four percent of the test section mass flow.

In the 0.3-m TCT facility, it is proposed to provide facilities for boundary-layer treatment in the form of 2-zone mass flow removal around the model and upstream of the model. This mass flow management will upset the basic thermodynamic balance of the tunnel, depending upon the mass bleed planned, and will thereby affect the basic tunnel controls.

In this report two basic methods of boundary-layer mass flow management have been considered. The first method is the passive bleed, to atmosphere, of the boundary-layer mass flow. The resulting mass/enthalpy unbalance is countered, either by a gas makeup scheme wherein makeup gas is required to be warmer than tunnel gas or by an extra liquid

nitrogen makeup scheme complemented by an electrical heater in the tunnel circuit. The second method is either to partially or fully reinject the boundary-layer mass flow into the tunnel circuit using an appropriately designed compressor/fan system.

All four schemes are workable, but have varied degrees of performance limitations, energy consumptions, and capital cost requirements.

In the passive bleed to atmosphere scheme, the limitations are that tunnel pressure should be in excess of $(1 + 0.2\ M^2)^3$ atm. In the gas makeup scheme the gas storage should be in excess of tunnel pressure and should have large volumetric capacity to maintain source pressure always higher than tunnel pressure. A mass flow control valve is also necessary. In the case of the liquid makeup scheme, a heater of nearly 1600 kW is required with its controls. However, no gas handling equipment is necessary in the liquid makeup scheme. In both the passive bleed schemes the net consumption of nitrogen is the same, and probably exceeds that of the recirculation schemes.

In the recirculation schemes, design of a fan/compressor capable of handling the full range of mass flow and pressure ratios is difficult. Unless the fan design is efficient, passive schemes would be superior. In a well-designed fan system, the energy consumption and liquid nitrogen consumption are lower. However, large gas management ducts, valves, etc. are needed, thereby increasing the capital costs. The tunnel controls can function properly.

In summary, the heater scheme with liquid nitrogen makeup is the simplest scheme, but consumes considerably more energy than an efficient recirculation scheme. However, there are no truncations in its performance, which are likely to occur in simple recirculation schemes.

In conclusion, any boundary-layer treatment scheme used to improve the flow field around the model is likely to affect the tunnel thermodynamic balance. Analysis must be made to account for both mass and enthalpy imbalances. The existing tunnel controls will function satisfactorily as long as a positive margin of mass and enthalpy is insured in measures which counter effects of boundary-layer treatment.

APPENDIX

FLOW CHART FOR BOUNDARY LAYER BLEED CONTROL

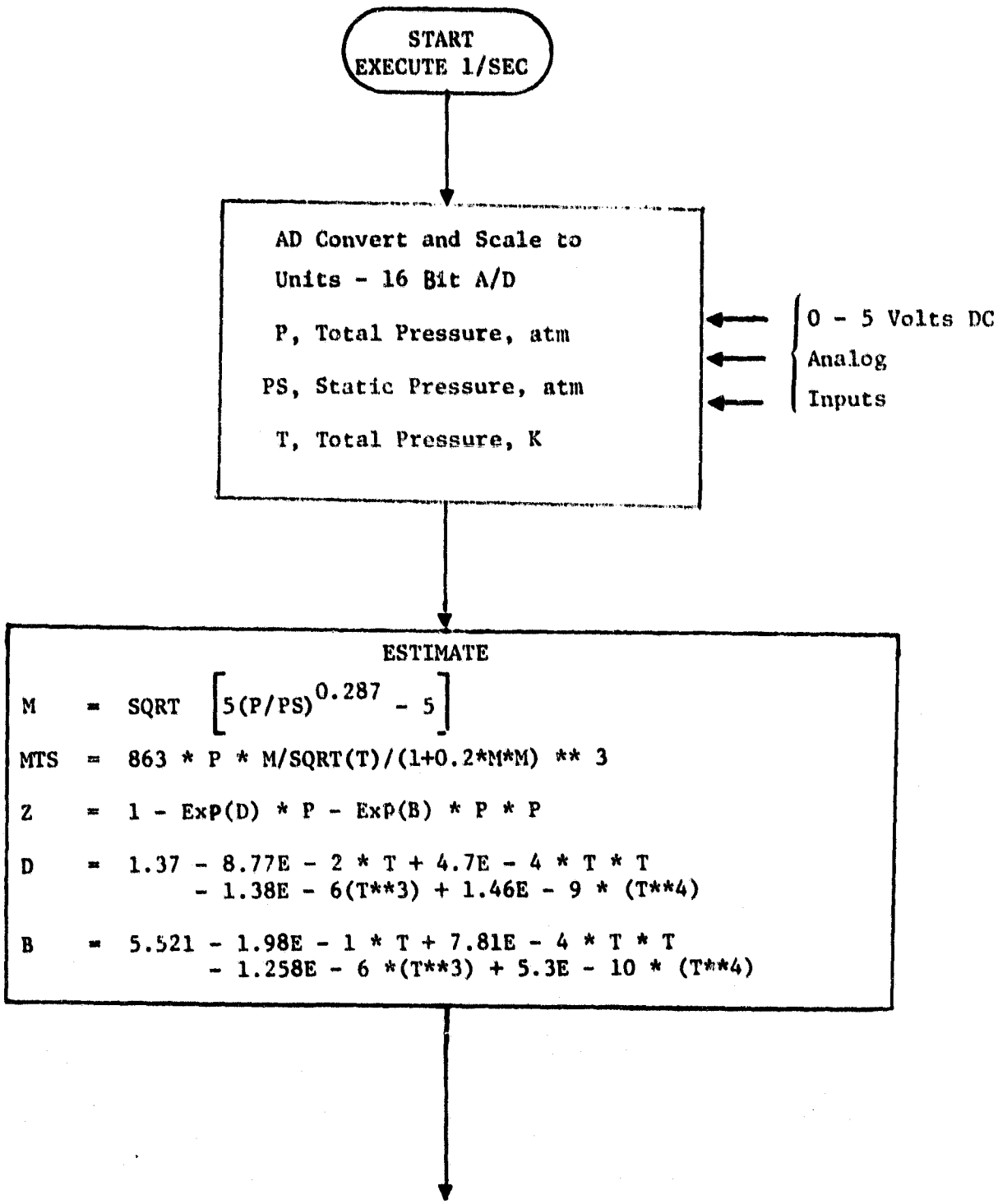

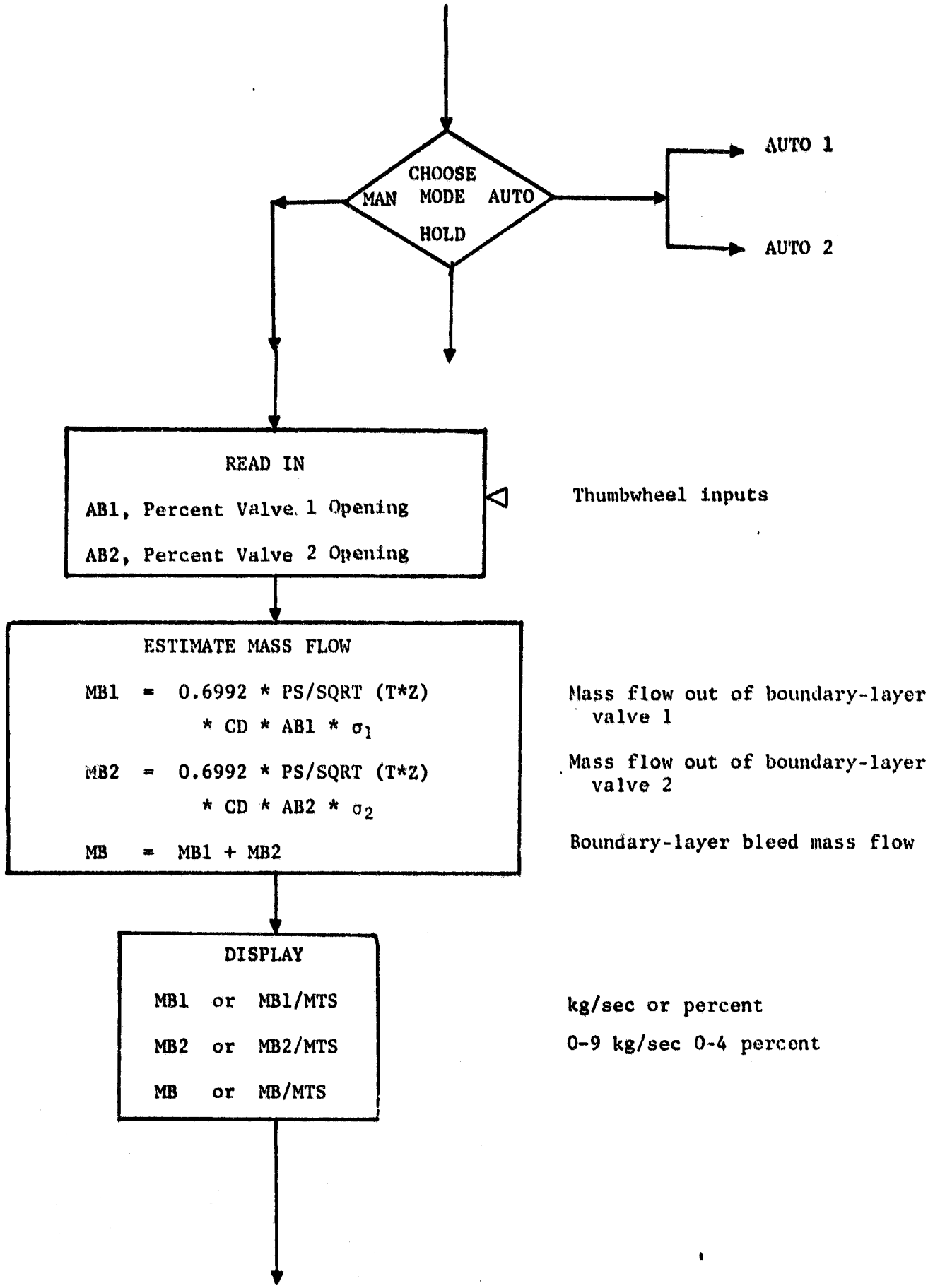
CHOOSE
MAN MODE AUTO
HOLD
AUTO 1
AUTO 2
READ IN
AB1, Percent Valve 1 Opening
AB2, Percent Valve 2 Opening
Thumbwheel inputs
ESTIMATE MASS FLOW
MB1 = 0.6992 * PS/SQRT (T*Z)
* CD * AB1 * σ1
MB2 = 0.6992 * PS/SQRT (T*Z)
* CD * AB2 * σ2
MB = MB1 + MB2
Mass flow out of boundary-layer valve 1
Mass flow out of boundary-layer valve 2
Boundary-layer bleed mass flow
DISPLAY
MB1 or MB1/MTS
MB2 or MB2/MTS
MB or MB/MTS
kg/sec or percent
0-9 kg/sec 0-4 percent

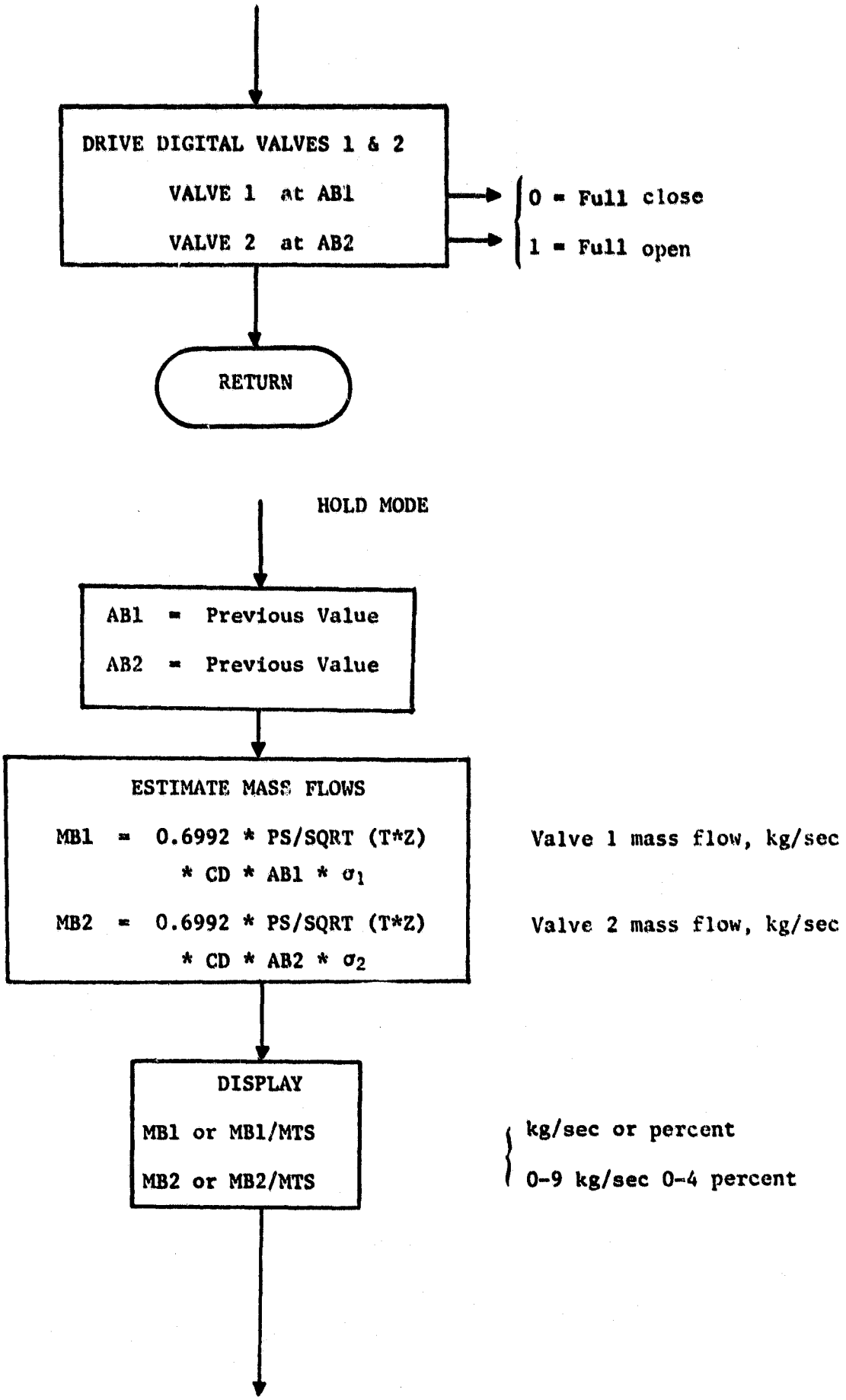
DRIVE DIGITAL VALVES 1 & 2
VALVE 1 at AB1
VALVE 2 at AB2
0 = Full close
1 = Full open
RETURN
HOLD MODE
AB1 = Previous Value
AB2 = Previous Value
ESTIMATE MASS FLOWS
MB1 = 0.6992 * PS/SQRT (T*Z) * CD * AB1 * σ1
Valve 1 mass flow, kg/sec
MB2 = 0.6992 * PS/SQRT (T*Z) * CD * AB2 * σ2
Valve 2 mass flow, kg/sec
DISPLAY
MB1 or MB1/MTS
MB2 or MB2/MTS
kg/sec or percent
0-9 kg/sec 0-4 percent

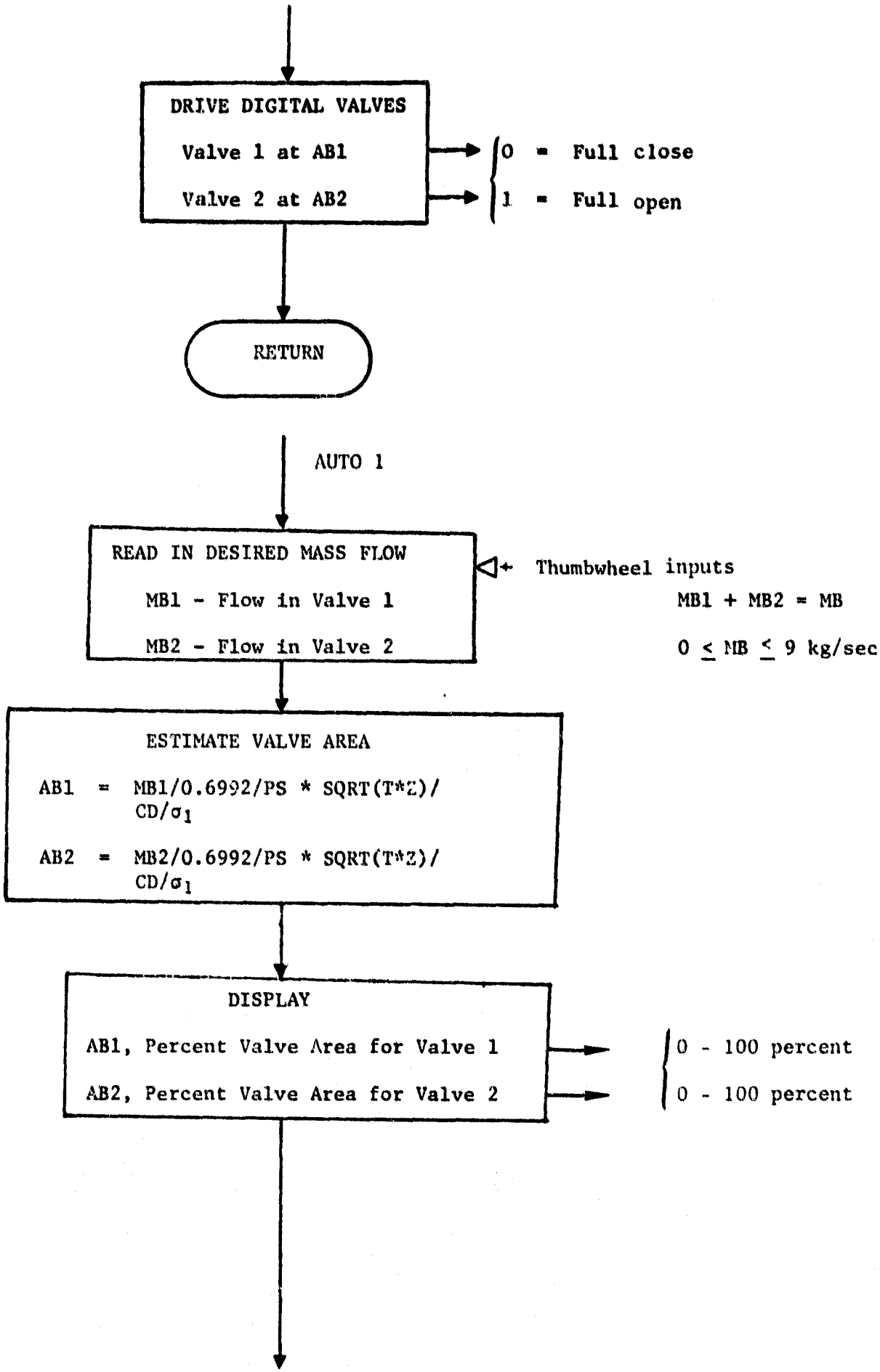
DRIVE DIGITAL VALVES
Valve 1 at AB1
Valve 2 at AB2
0 = Full close
1 = Full open
RETURN
AUTO 1
READ IN DESIRED MASS FLOW
MB1 - Flow in Valve 1
MB2 - Flow in Valve 2
Thumbwheel inputs
MB1 + MB2 = MB
0 ≤ MB ≤ 9 kg/sec
ESTIMATE VALVE AREA
AB1 = MB1/0.6992/PS * SQRT(T*Z)/ CD/σ1
AB2 = MB2/0.6992/PS * SQRT(T*Z)/ CD/σ1
DISPLAY
AB1, Percent Valve Area for Valve 1
AB2, Percent Valve Area for Valve 2
0 - 100 percent
0 - 100 percent

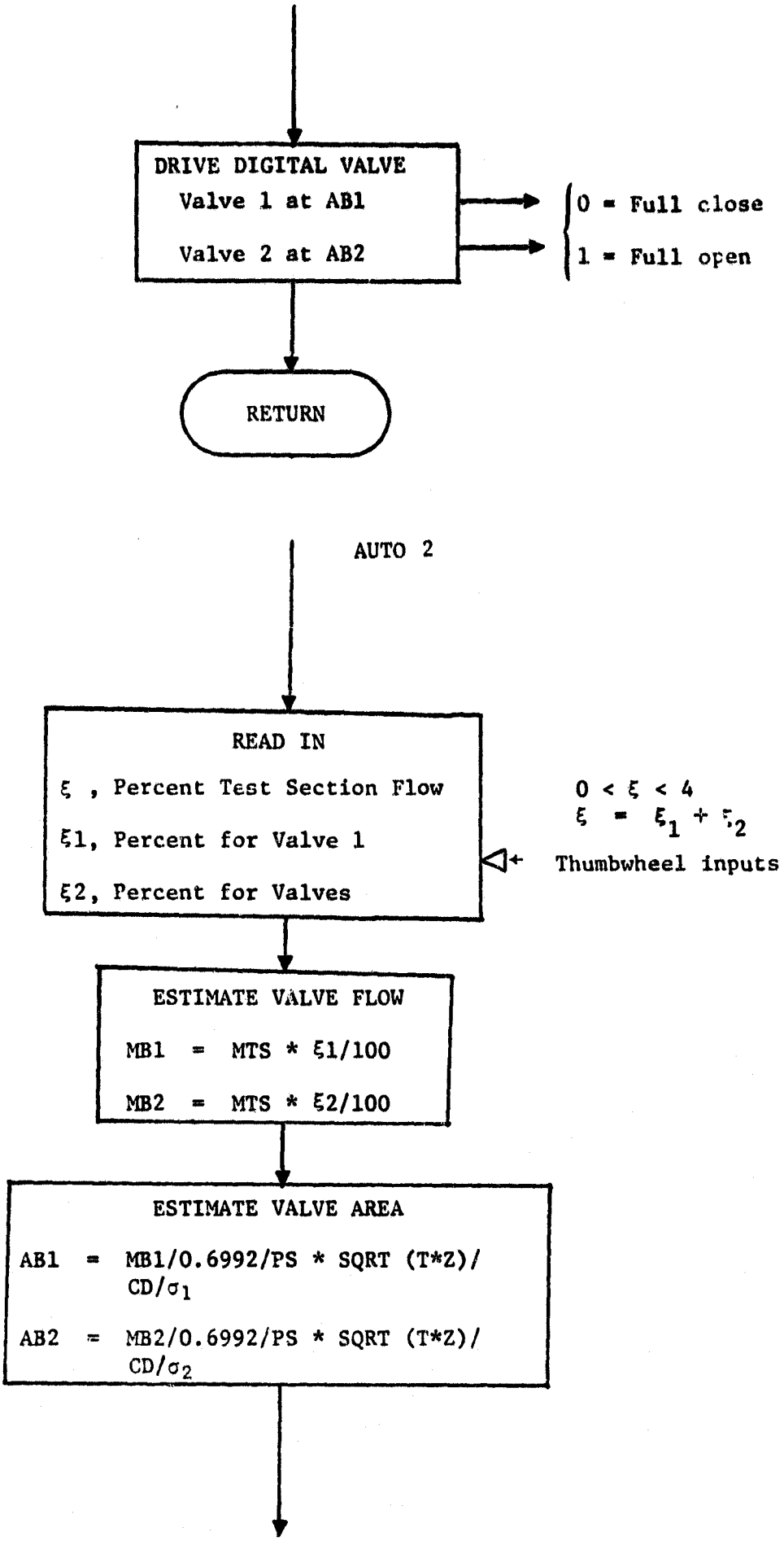
DRIVE DIGITAL VALVE
Valve 1 at AB1
Valve 2 at AB2
0 = Full close
1 = Full open
RETURN
AUTO 2
READ IN
ξ , Percent Test Section Flow
ξ1, Percent for Valve 1
ξ2, Percent for Valves
0 < ξ < 4
ξ = ξ1 + ξ2
Thumbwheel inputs
ESTIMATE VALVE FLOW
MB1 = MTS * ξ1/100
MB2 = MTS * ξ2/100
ESTIMATE VALVE AREA
AB1 = MB1/0.6992/PS * SQRT (T*Z)/ CD/σ1
AB2 = MB2/0.6992/PS * SQRT (T*Z)/ CD/σ2

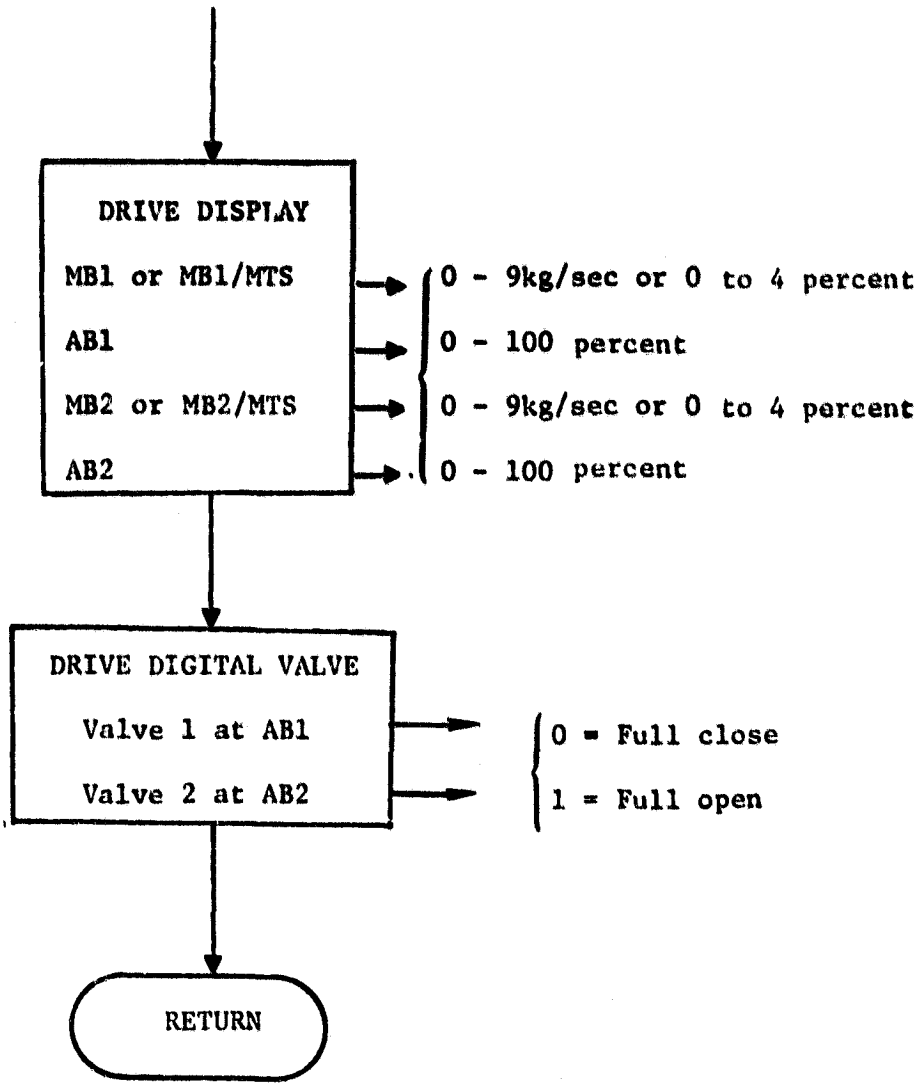
DRIVE DISPLAY
MB1 or MB1/MTS
AB1
MB2 or MB2/MTS
AB2
0 - 9kg/sec or 0 to 4 percent
0 - 100 percent
0 - 9kg/sec or 0 to 4 percent
0 - 100 percent
DRIVE DIGITAL VALVE
Valve 1 at AB1
Valve 2 at AB2
0 = Full close
1 = Full open
RETURN

COEFFICIENT DEFINITIONS, PANEL CONTROLS AND DISPLAYS

COEFFICIENTS

CD = Full open area valve coefficient for the boundary-layer bleed valves

σ_1, σ_2 = Valve flow asymmetry factors to accommodate turning mass flow, $0.9 \leq \sigma_1, \sigma_2 \leq 1.1$

z = Compressibility factor defined by parameters B, D, and variables P and T

MB, MTS = Mass flow rates for boundary layer and test section

ξ = Percentage of boundary-layer mass flow normalized to test section flow, = $\epsilon \times 100$

PANEL CONTROLS

Area control thumbwheels 0.00 to 99.9 percent mass flow control thumbwheel, 0.00 to 10.0 kg/sec percent mass flow control thumbwheel, 0.00 to 4.00 mode switches.

DISPLAYS

Valve area = 0 to 100 percent

Valve flow = 0 to 10 kg/sec

Valve flow = 0 to 4 percent of test section flow

REFERENCES

1. Balakrishna, S.: Synthesis of a Control Model for a Liquid Nitrogen Cooled, Closed-Circuit, Cryogenic Nitrogen Wind Tunnel and Its Validation. NASA-CR-162508, Feb. 1980.

2. Balakrishna, S.: Automatic Control of a Liquid Nitrogen Cooled, Closed-Circuit, Cryogenic, Pressure Tunnel. Progress Report for NASA Grant NSG-1503, NASA CR-162636, March 1980.

3. Balakrishna, S.: Minimum Energy Test Direction Design in the Control of Cryogenic Wind Tunnels. Progress Report for NASA Grant NSG-1503, NASA CR-163244, June 1980.

4. Strett, C.L: A Method for Computing Boundary Layer Growth on a Perforated Suction Surface. Master's Thesis submitted to Ohio State University, May 1979.

5. Kilgore, R.A.: Goodyer, M.J.; Adcock, J.B.; and Davenport, E.E.: The Cryogenic Wind Tunnel Concept for High Reynolds Number Testing. NASA TN D-7762, Nov. 1974.

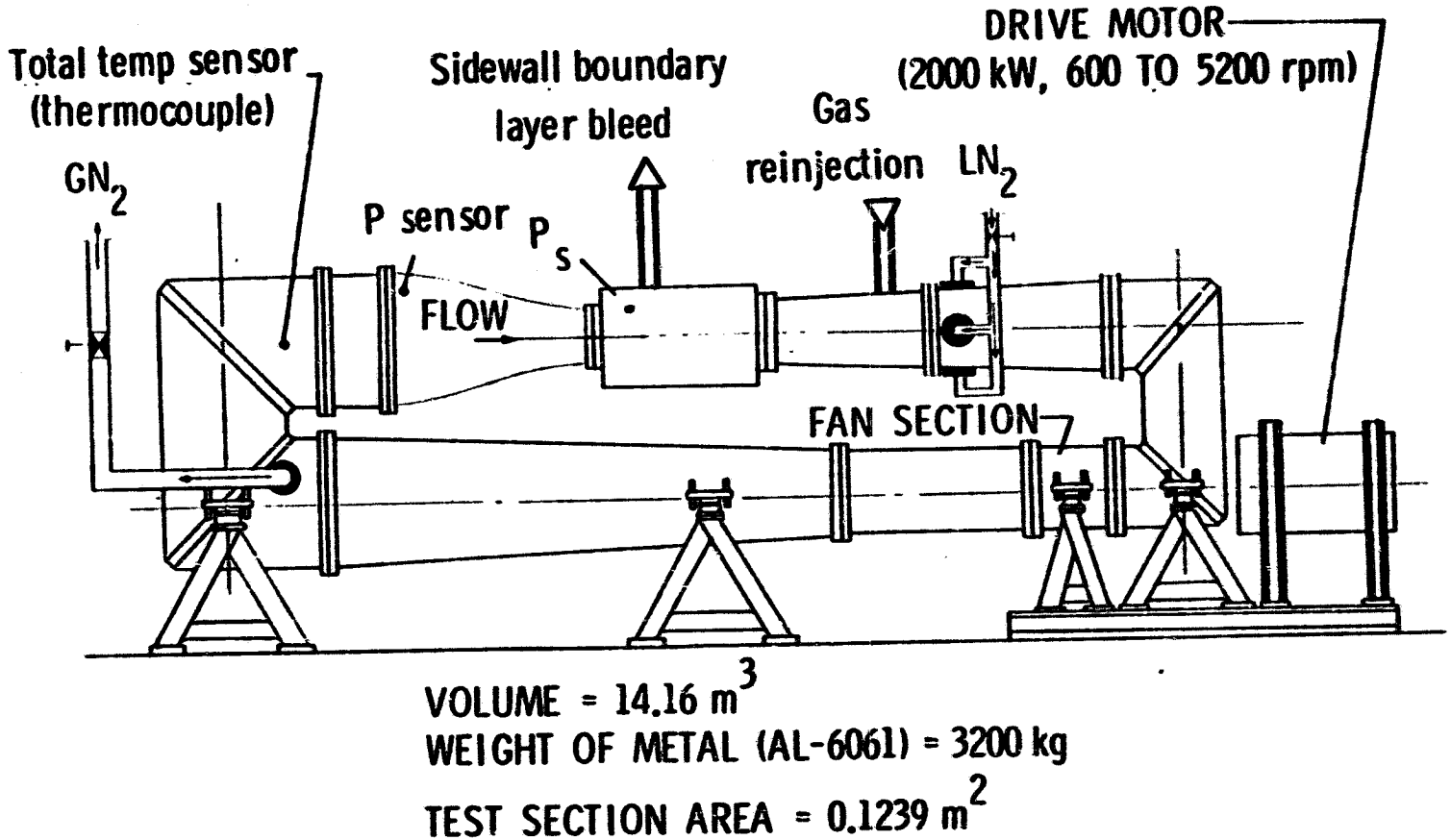

Figure 1. Configuration of the 0.3-m TCT.

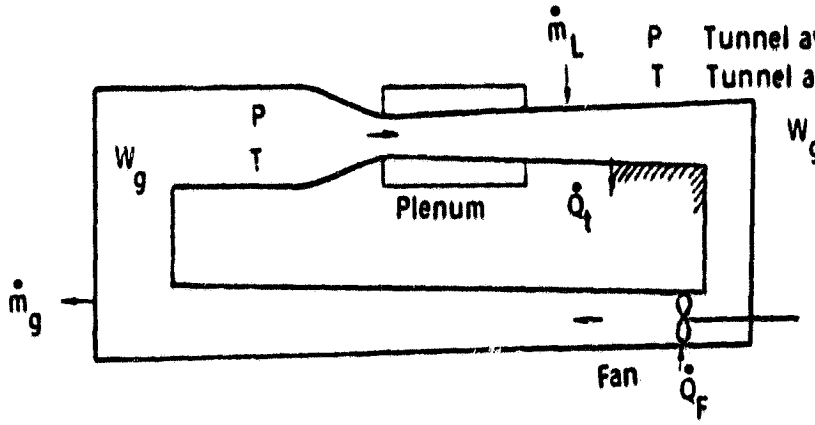

Assumptions

Perfect gas behavior
Uniform tunnel temperature
Work, potential & kinetic energy ignored

first law of thermodynamics $$-\dot{Q}_t + \dot{Q}_F + \dot{m}_L h_L - \dot{m}_g h_g = W_g C_v \frac{dT}{dt} + u(\dot{m}_L - \dot{m}_g)$$

Where

h_L Liquid nitrogen enthalpy J/kg

u Specific internal energy

h_g Gas enthalpy J/kg

$\dot{Q}_t$ Heat flow to tunnel metal wall J/sec

$\dot{Q}_F$ Heat flow from Fan operation J/sec

$\dot{m}_g$ Gaseous nitrogen bleed kg/sec

$\dot{m}_L$ Liquid nitrogen mass flow kg/sec

Figure 2. Thermodynamic model of a cryogenic tunnel.

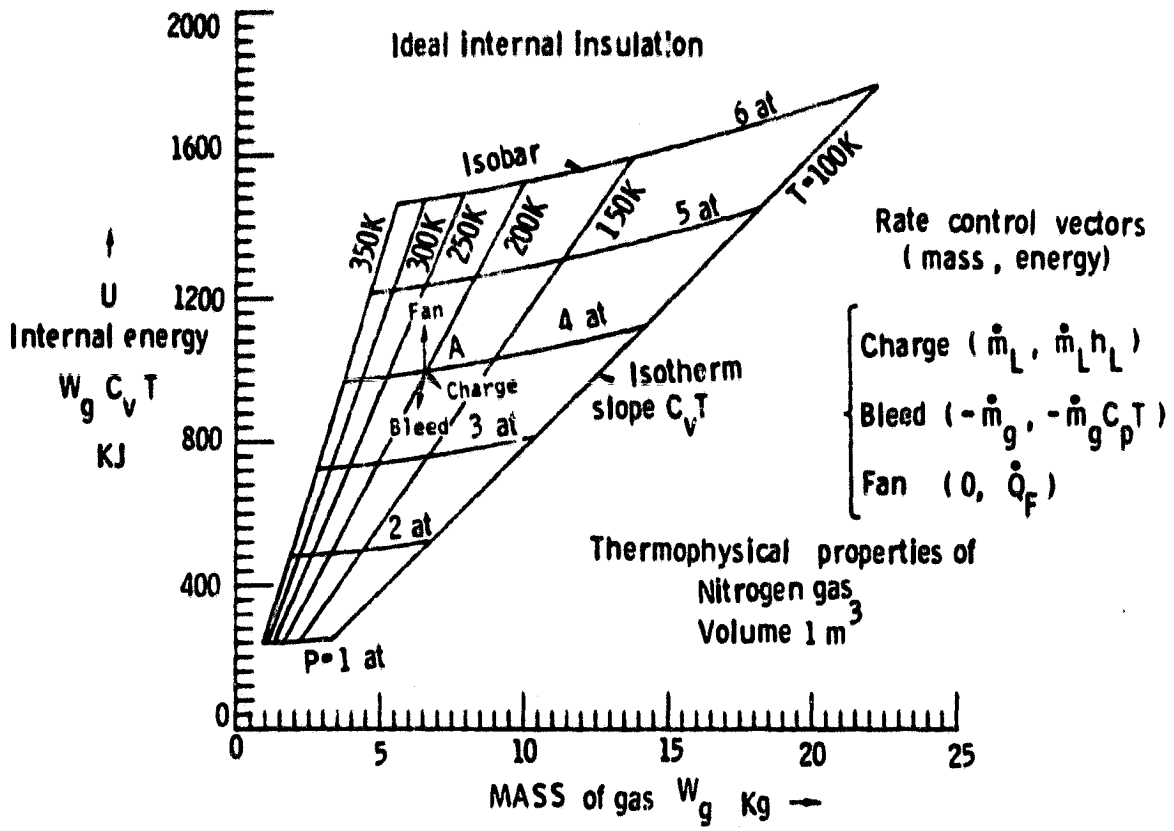

Figure 3. Energy state diagram.

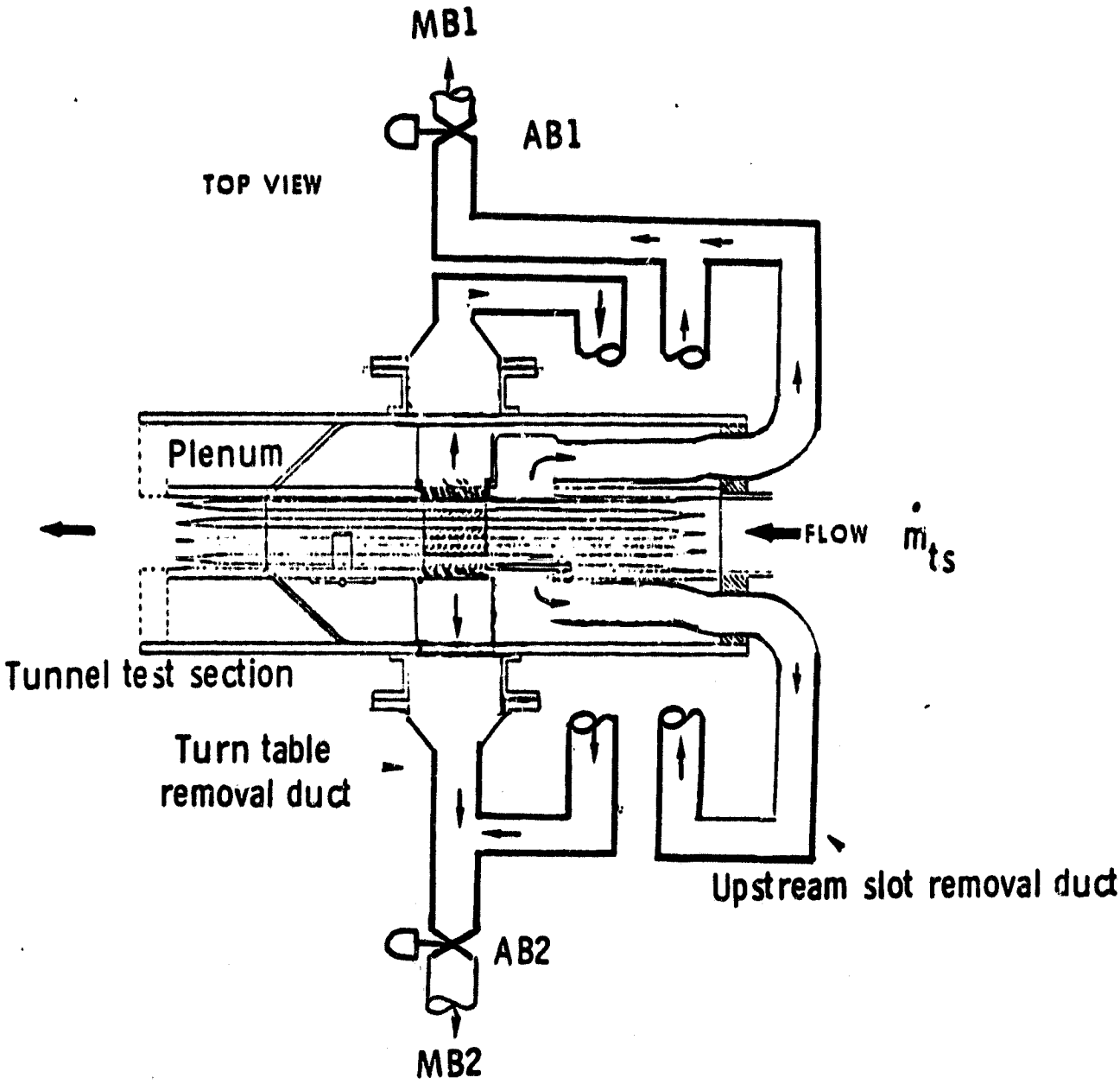

Figure 4. Test section and boundary-layer removal valves.

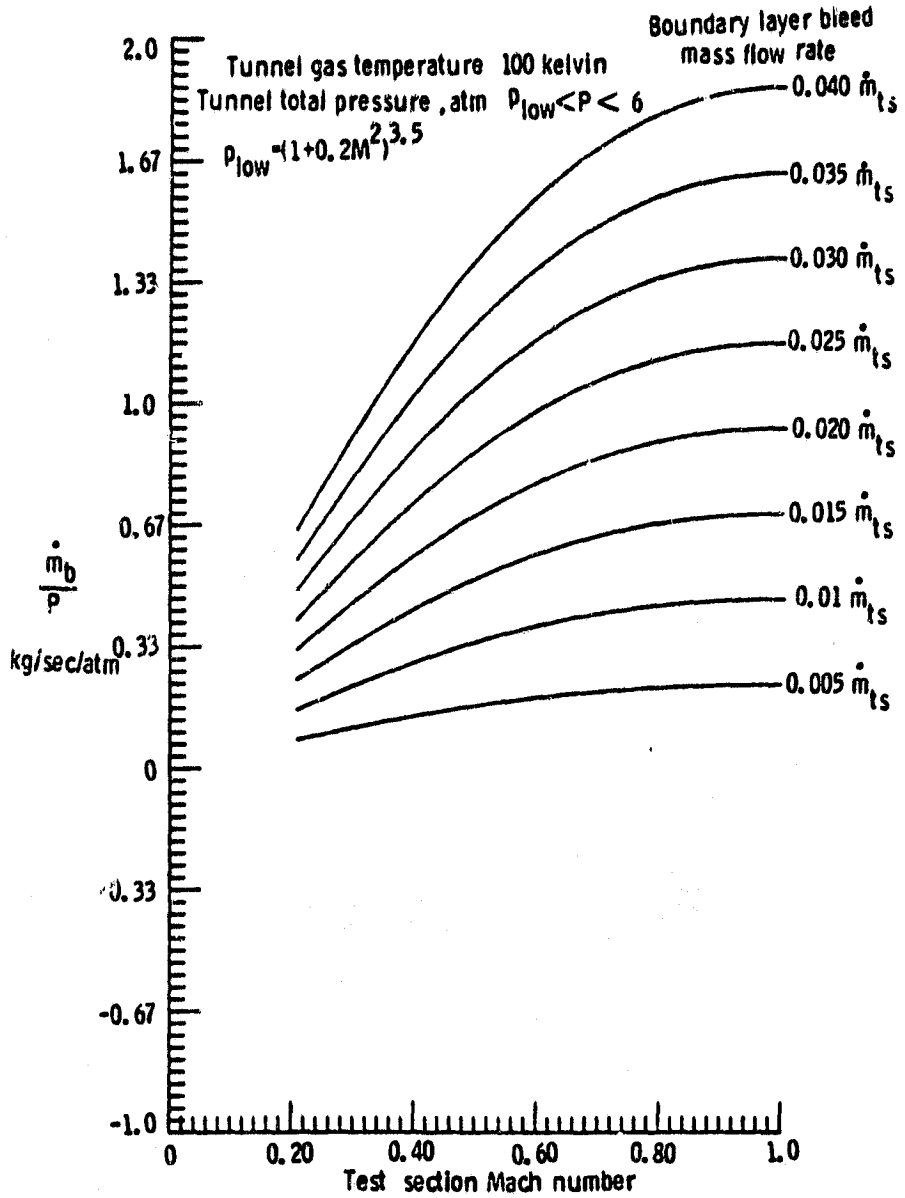

Figure 5. Loci of boundary-layer bleed mass flow, 100 K.

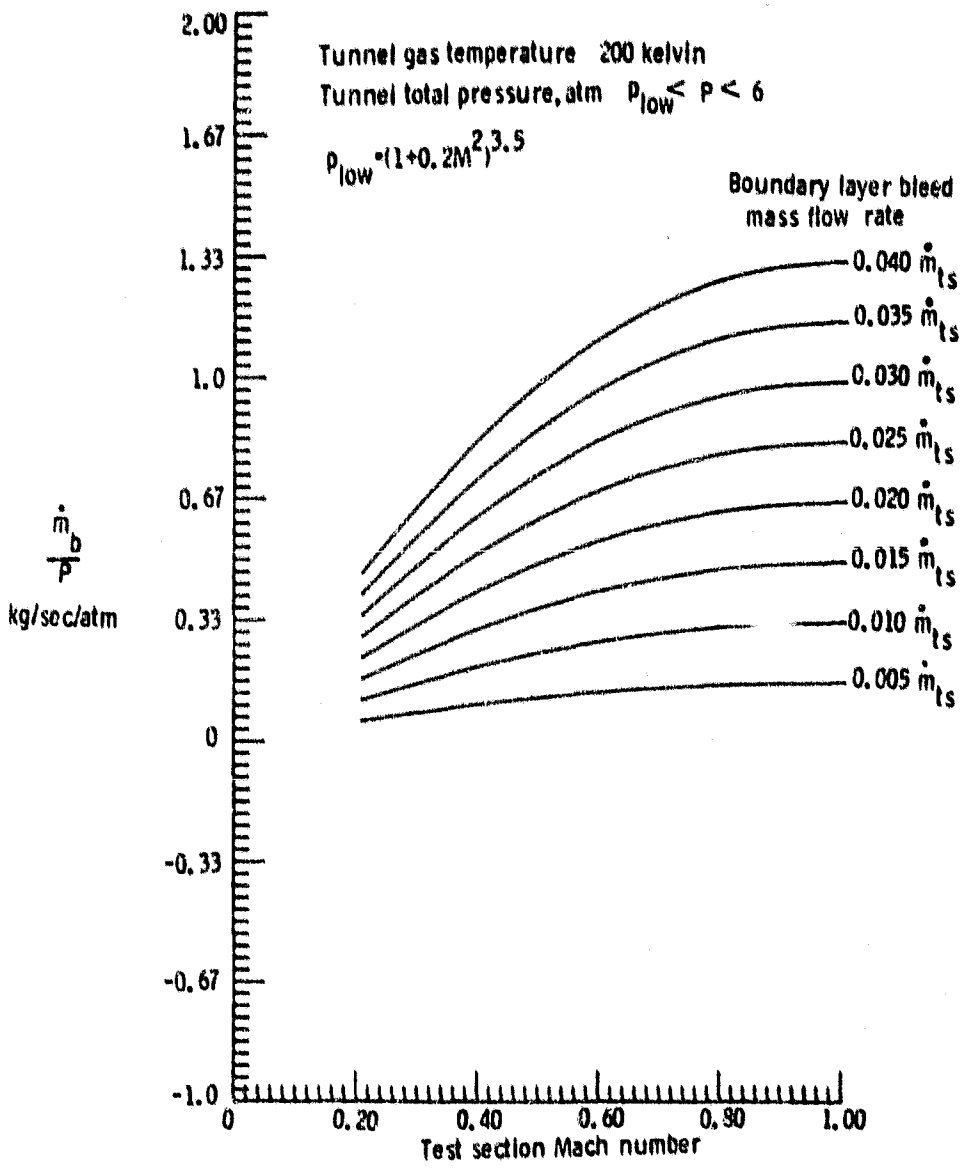

Figure 6. Loci of boundary-layer bleed mass flow, 200 K.

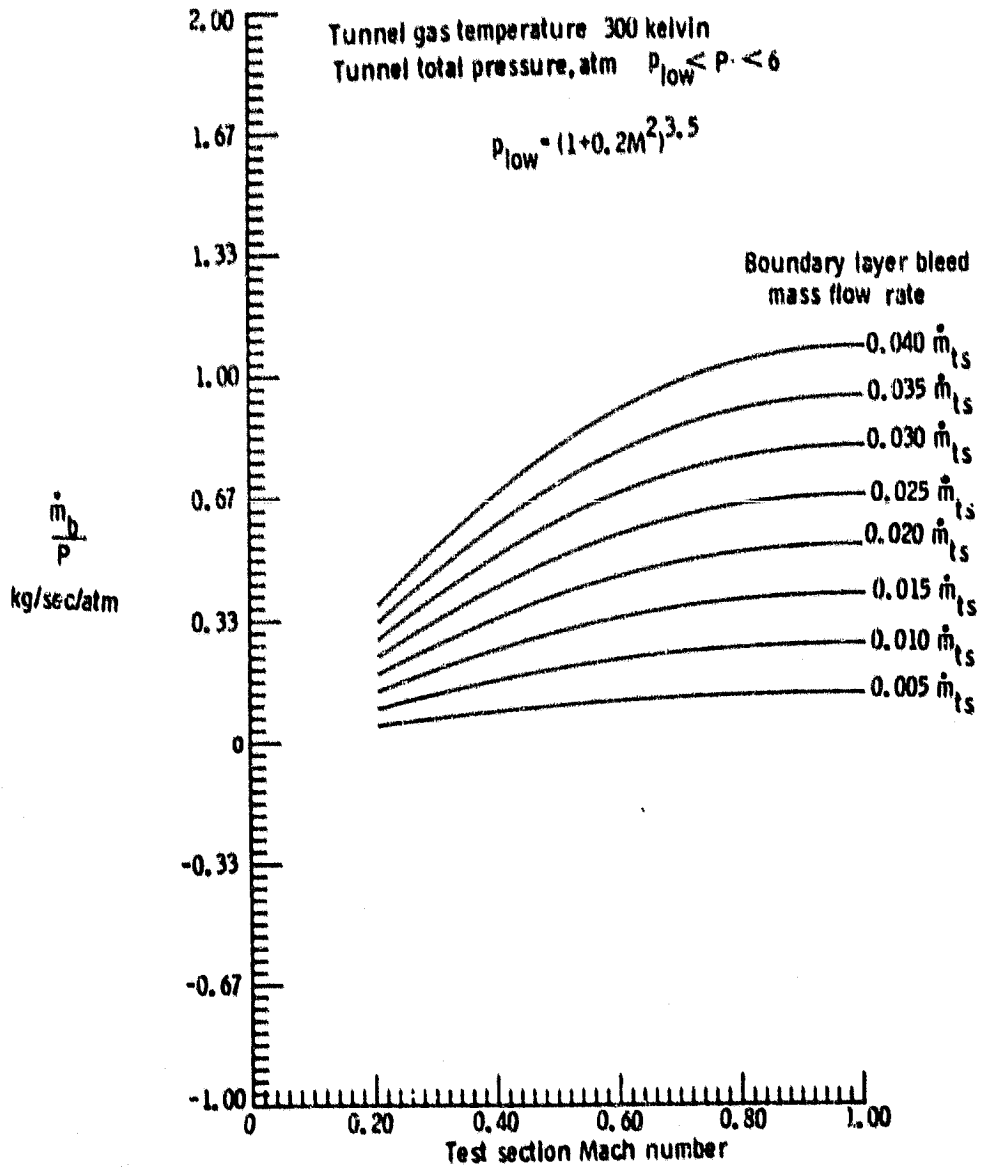

Figure 7. Loci of boundary-layer bleed mass flow, 300 K.

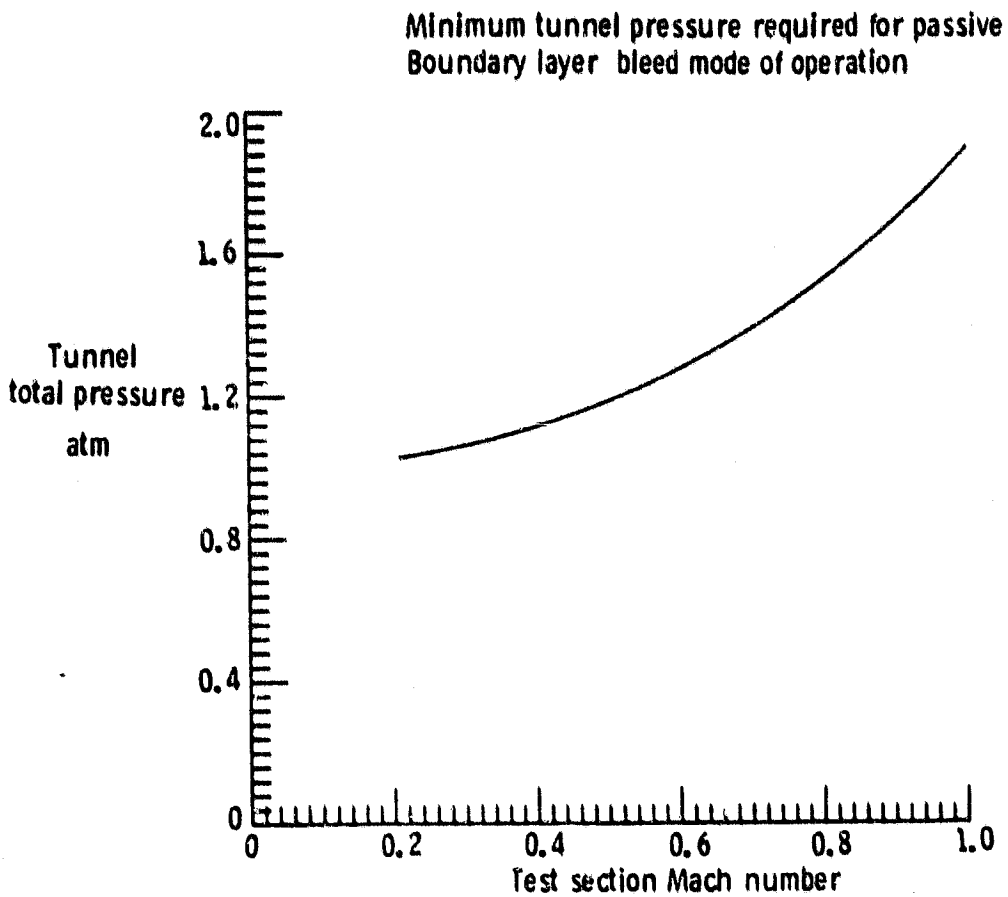

Figure 8. Minimum tunnel pressure required for passive boundary-layer bleed mode of operation.

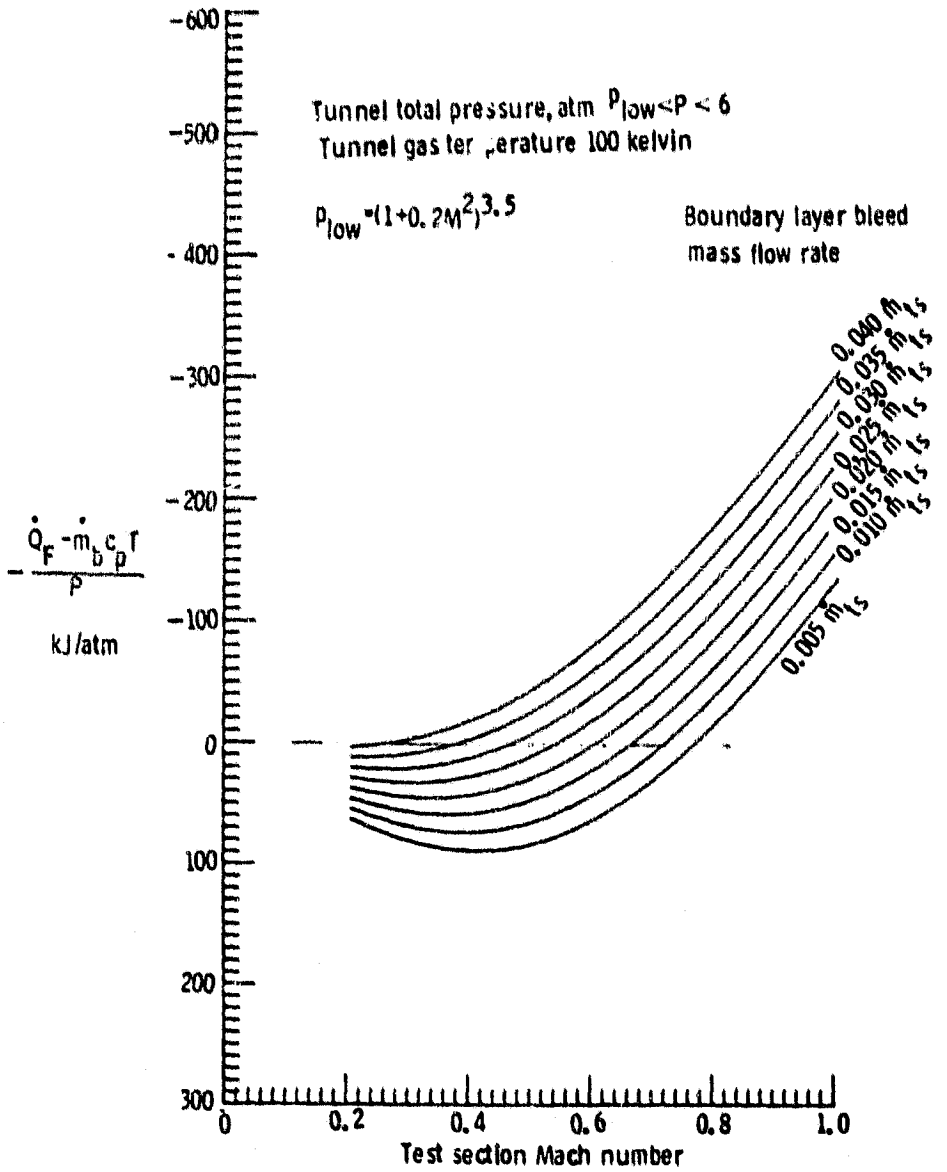

Figure 9. Loci of energy required for balanced cryogenic tunnel operation, 100 K.

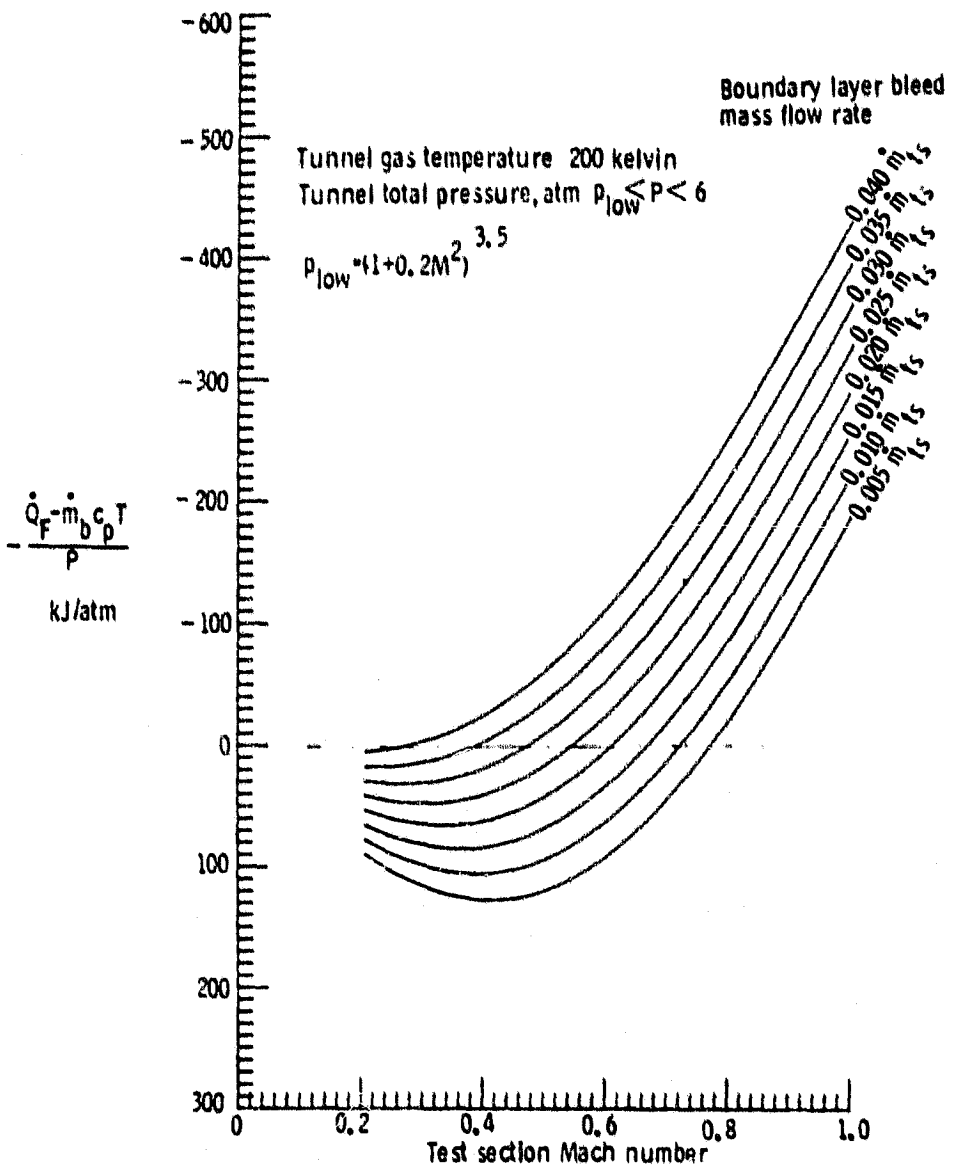

Figure 10. Loci of energy required for balanced cryogenic tunnel operation, 200 K.

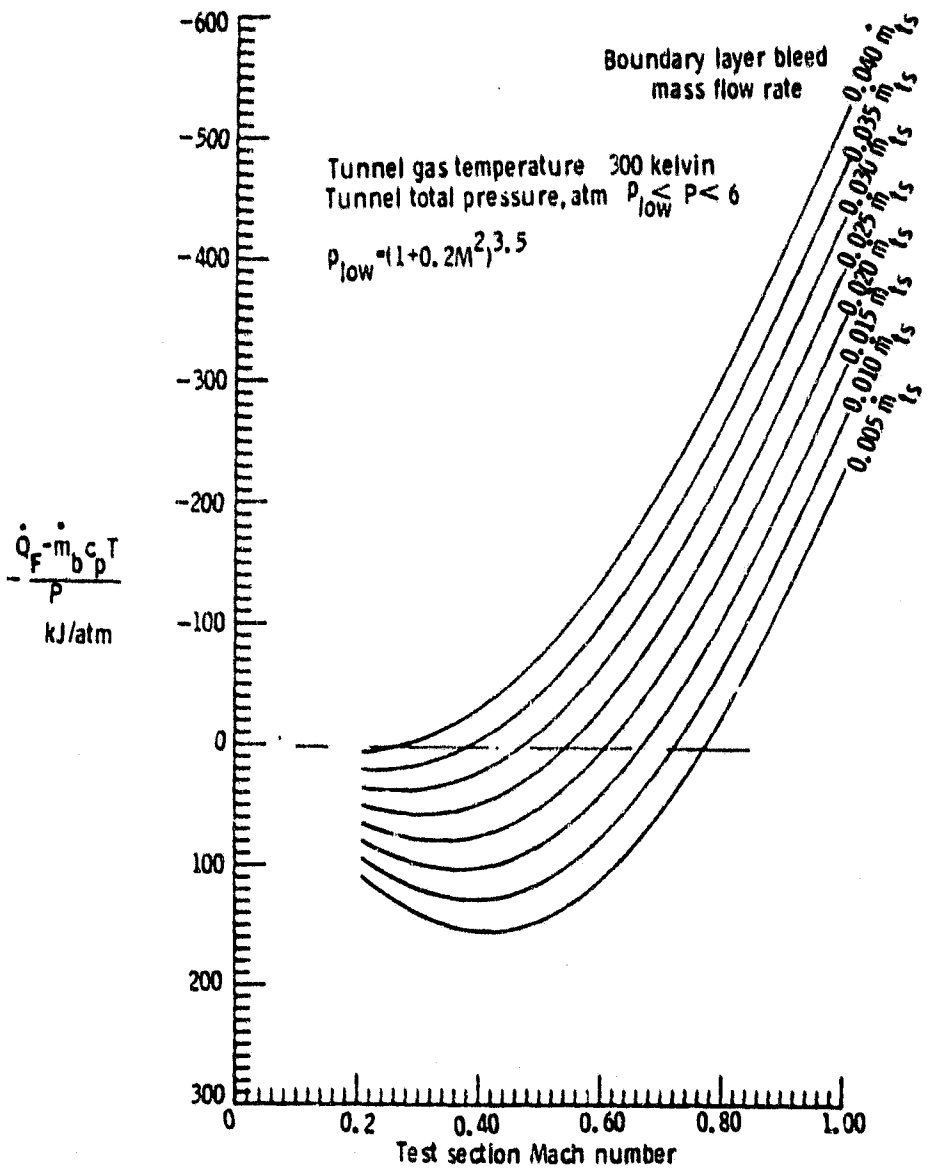

Figure 11. Loci of energy required for balanced cryogenic tunnel operation, 300 K.

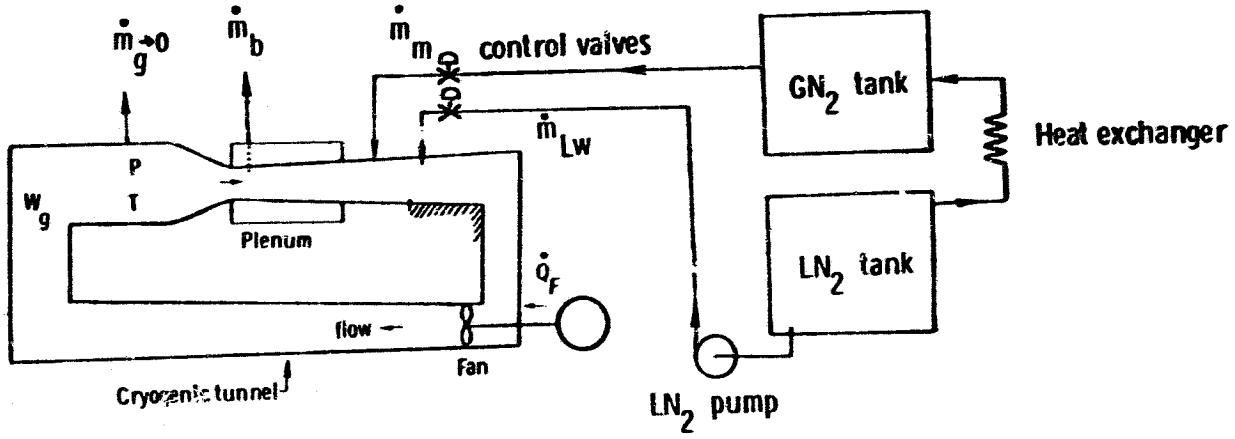

for themodynamic equilibrium

$$\dot{m}_{Lw} = \frac{-\dot{Q}_F}{h_L - c_F T} \qquad \dot{m}_b = \epsilon \dot{m}_{ts}$$

$$\dot{m}_b > \dot{m}_{Lw} \qquad \dot{m}_m = \dot{m}_b - \dot{m}_{Lw}$$

$$h_m = c_p T$$

Figure 12. Passive bleed boundary-layer control scheme, gas makeup.

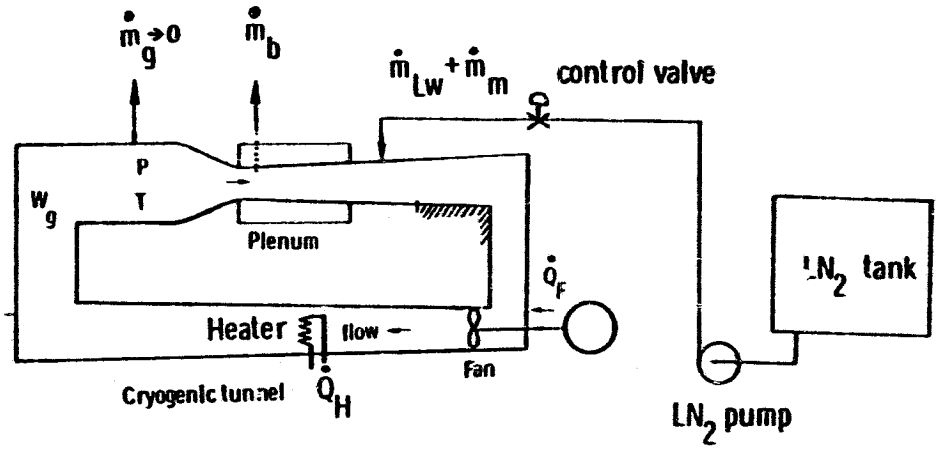

for thermodynamic equilibrium

$$\dot{m}_b > \dot{m}_{Lw} \qquad \dot{m}_b = \epsilon \dot{m}_{ts}$$

$$\dot{Q}_H = -\dot{m}_m (h_L - c_p T)$$

$$\dot{m}_m + \dot{m}_{Lw} = \frac{-(\dot{Q}_F + \dot{Q}_H)}{h_L - c_p T} \qquad \dot{m}_{Lw} = \frac{-\dot{Q}_F}{h_L - c_p T}$$

Figure 13. Passive bleed boundary-layer control scheme, liquid makeup.

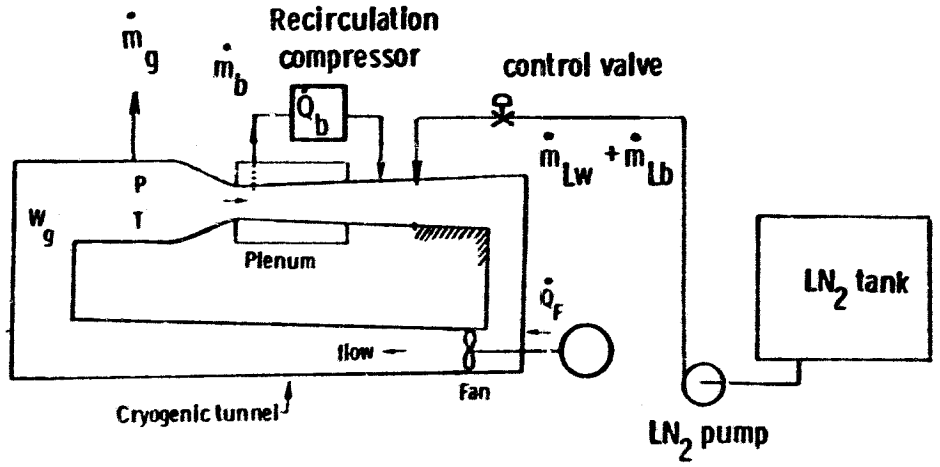

for thermodynamic equilibrium

$$\dot{m}_g = \dot{m}_{Lw} + \dot{m}_{Lb} \qquad \dot{m}_b = \epsilon \, \dot{m}_{ts}$$

$$\dot{m}_{Lw} + \dot{m}_{Lb} = \frac{-(\dot{Q}_F + \dot{Q}_b)}{h_L - c_p T}$$

$$\dot{Q}_b = \dot{m}_b \, c_p \, \delta T$$

Figure 14. Recirculation mode boundary-layer control.

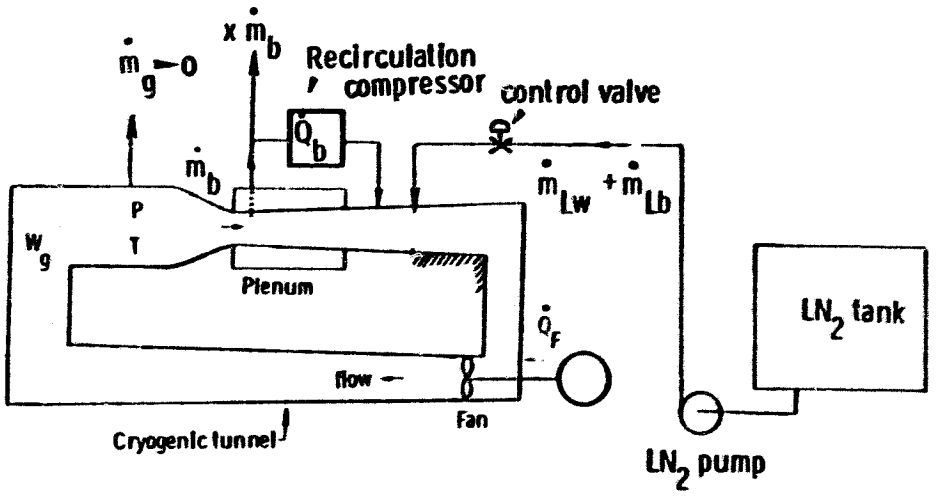

for thermodynamic equilibrium

$$x\,\dot{m}_b = \dot{m}_{Lw} + \dot{m}_{Lb} \qquad \dot{m}_b = \epsilon\,\dot{m}_{ts}$$

$$\dot{m}_{Lw} + \dot{m}_{Lb} = \frac{-(\dot{Q}_F + \dot{Q}_b)}{h_L - c_p T} \qquad \dot{m}_{Lb} = \frac{-\dot{Q}_b}{h_L - c_p T}$$

$$\dot{Q}_b = (1 - x)\,\dot{m}_b\, c_p \delta T$$

Figure 15. Partial recirculation mode boundary-layer control.

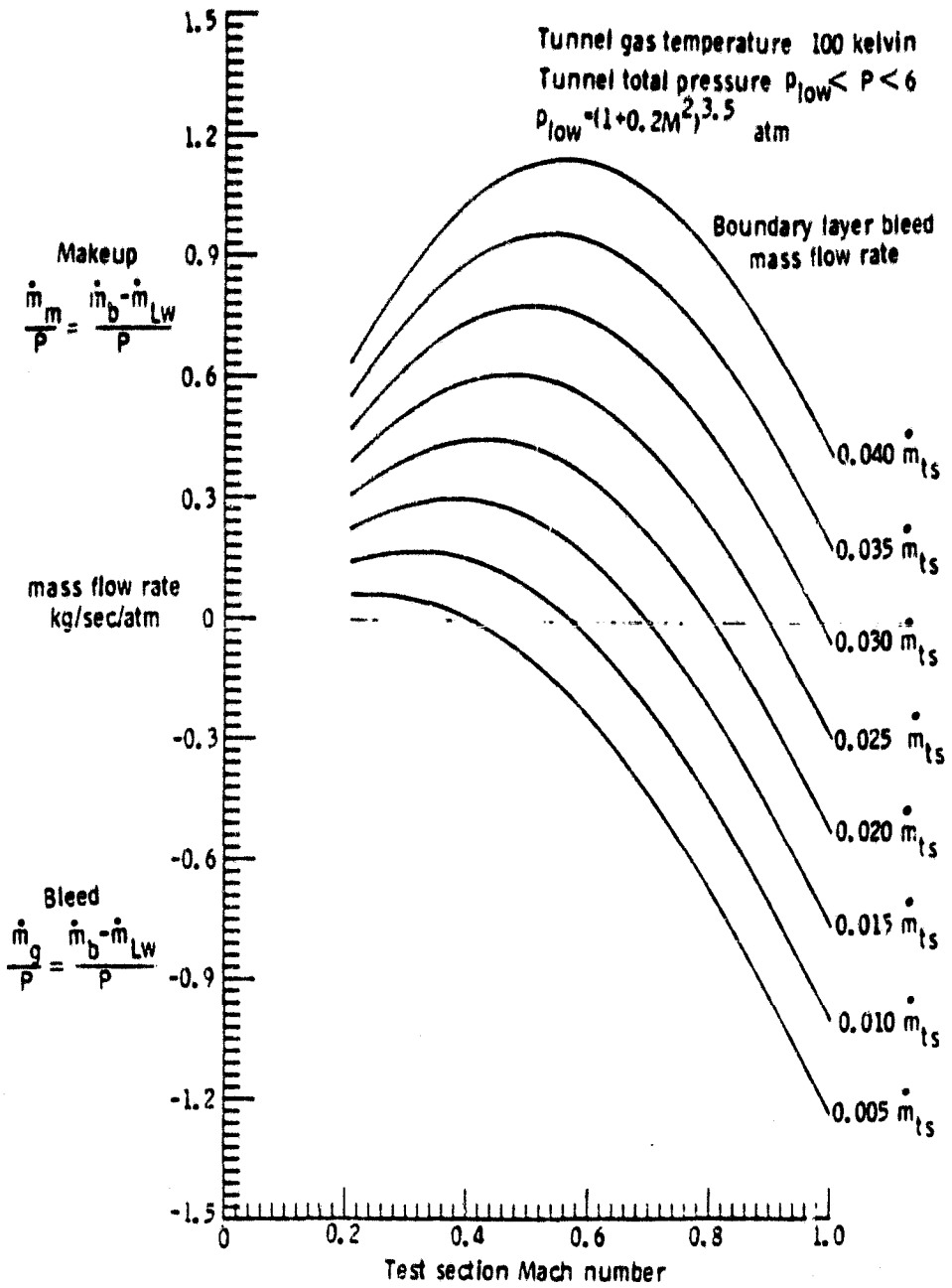

Figure 16. Makeup of mass flow loci, 100 K.

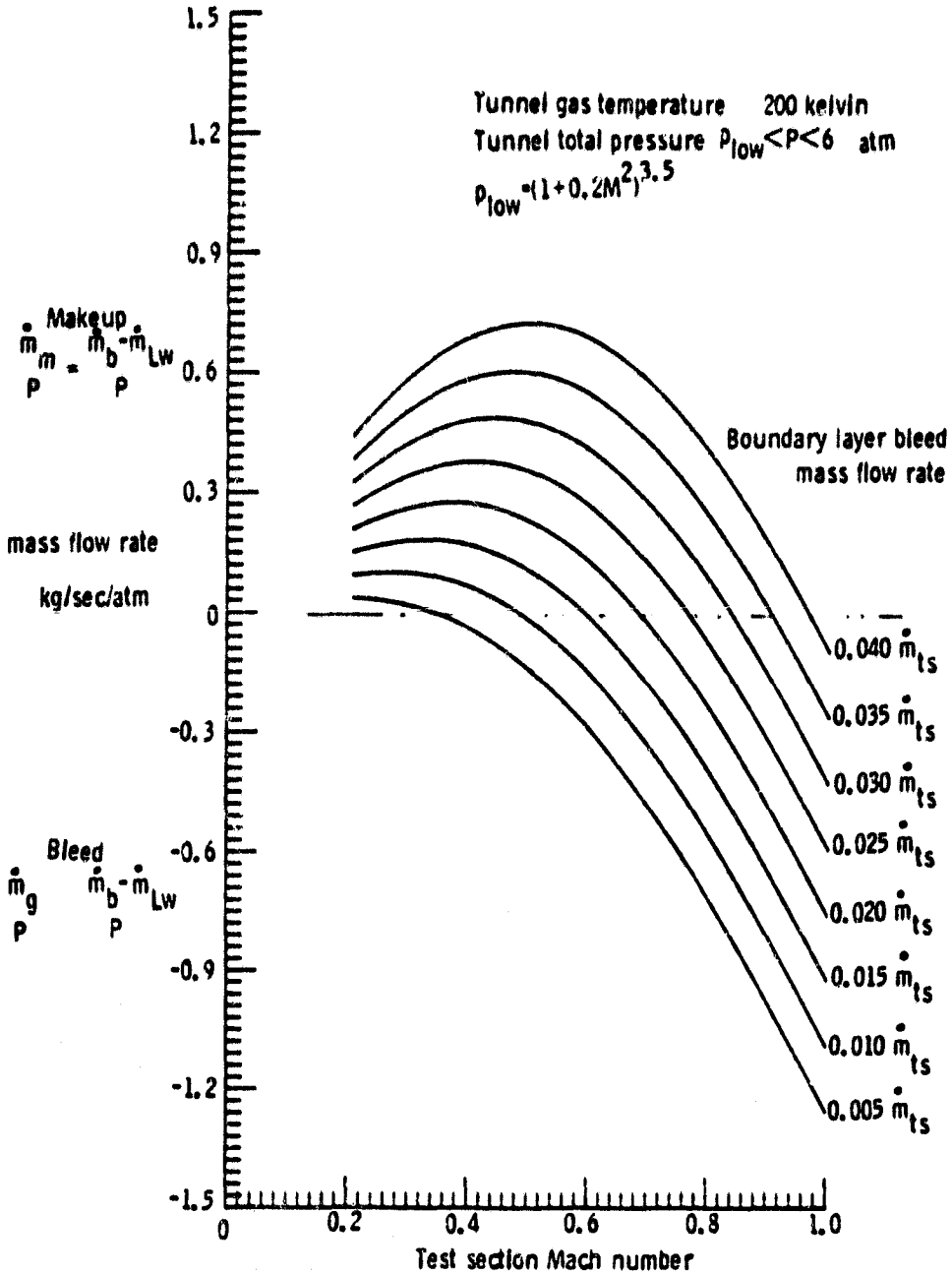

Figure 17. Makeup of mass flow loci, 200 K.

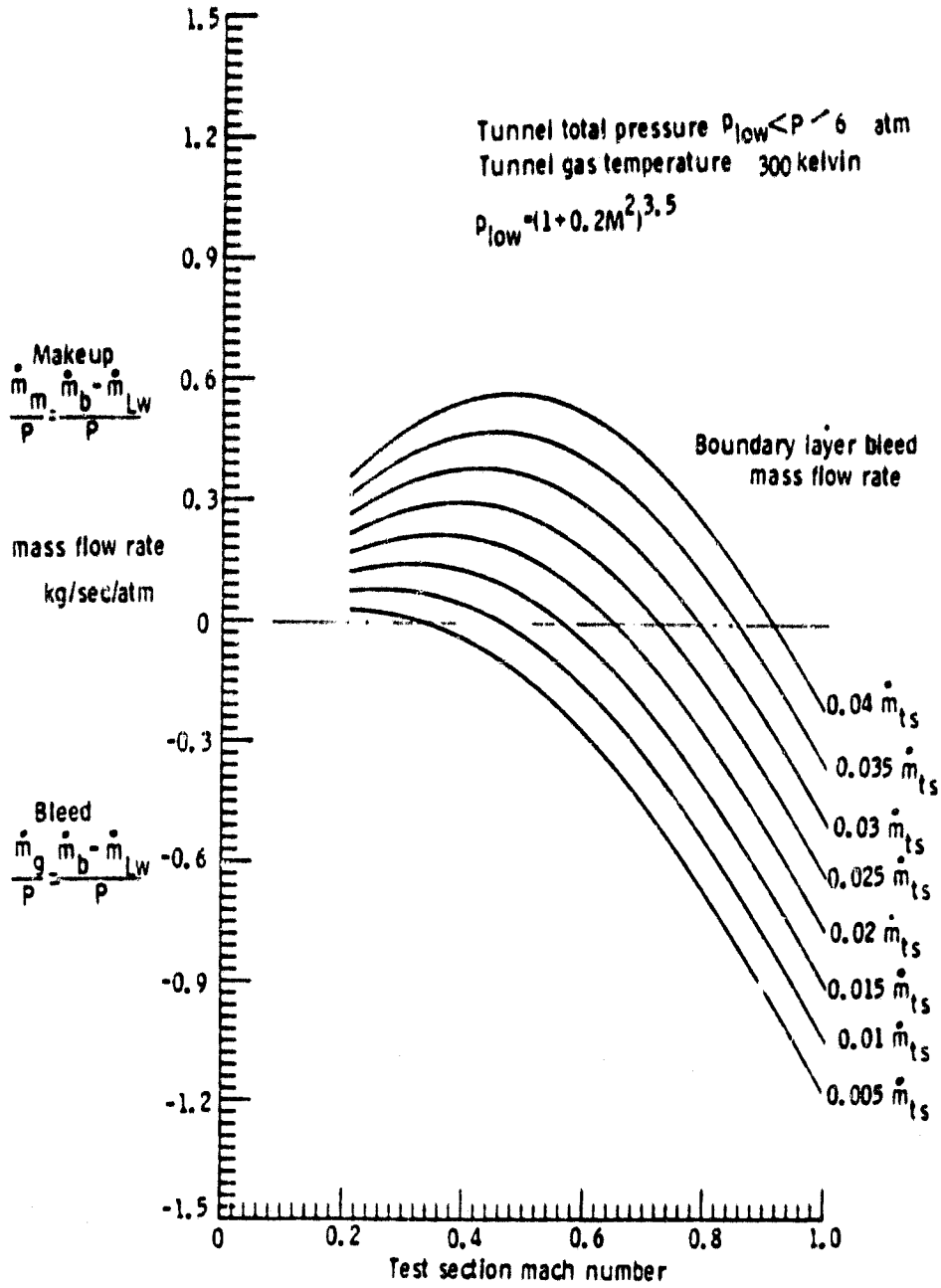

Figure 18. Makeup of mass flow loci, 300 K.

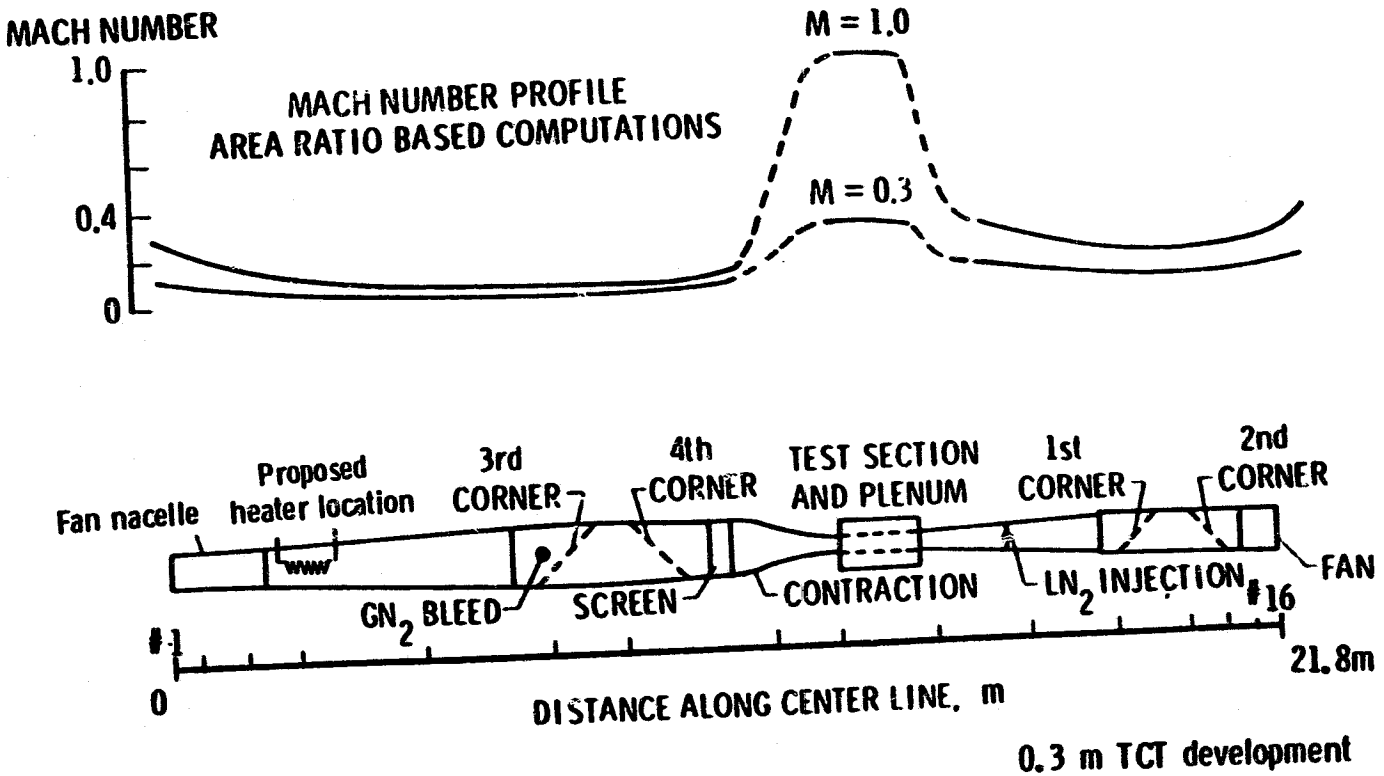

Figure 19. Spatial profile of tunnel flow Mach number.

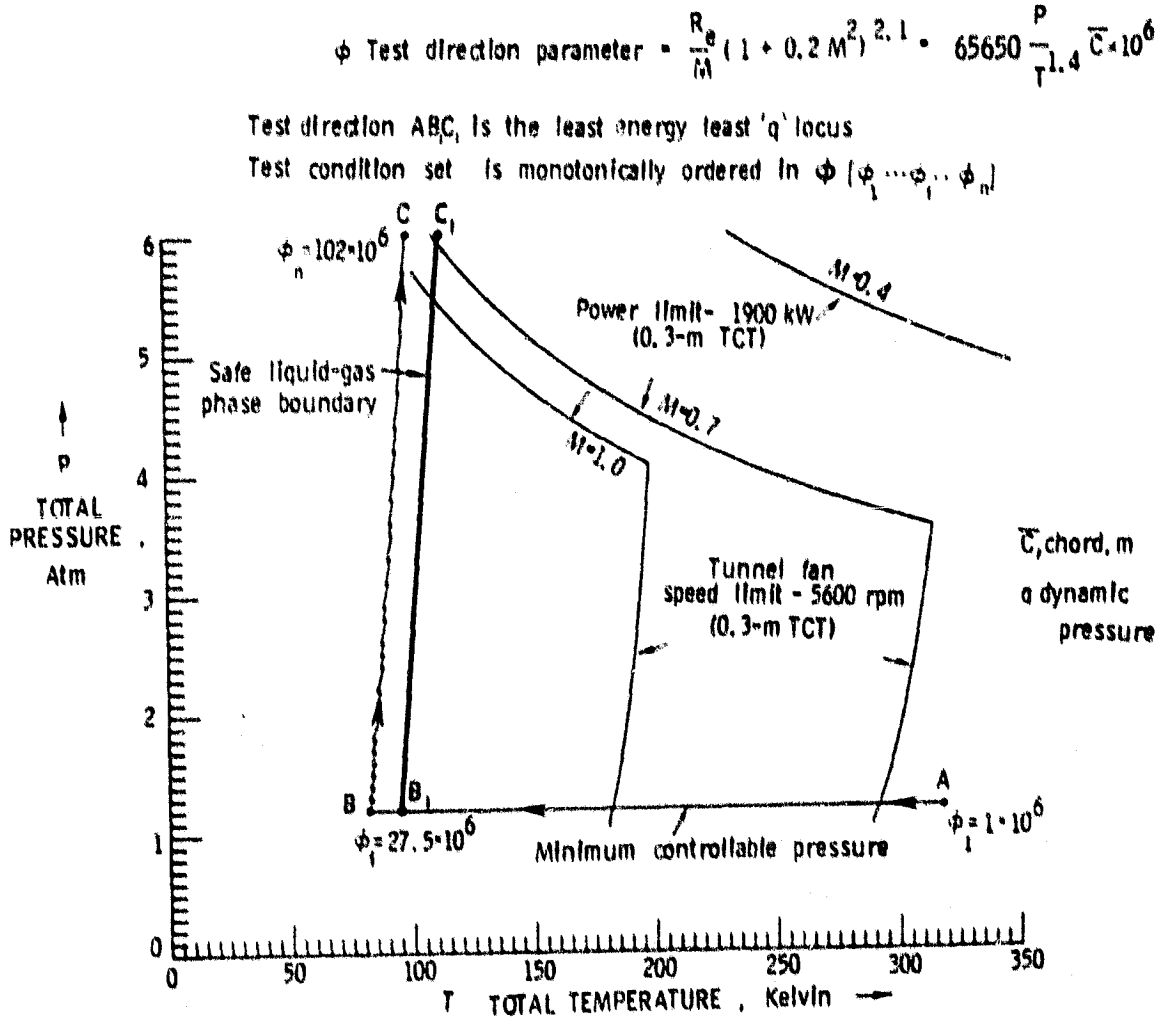

Figure 20. Test direction design—least energy consumption locus.

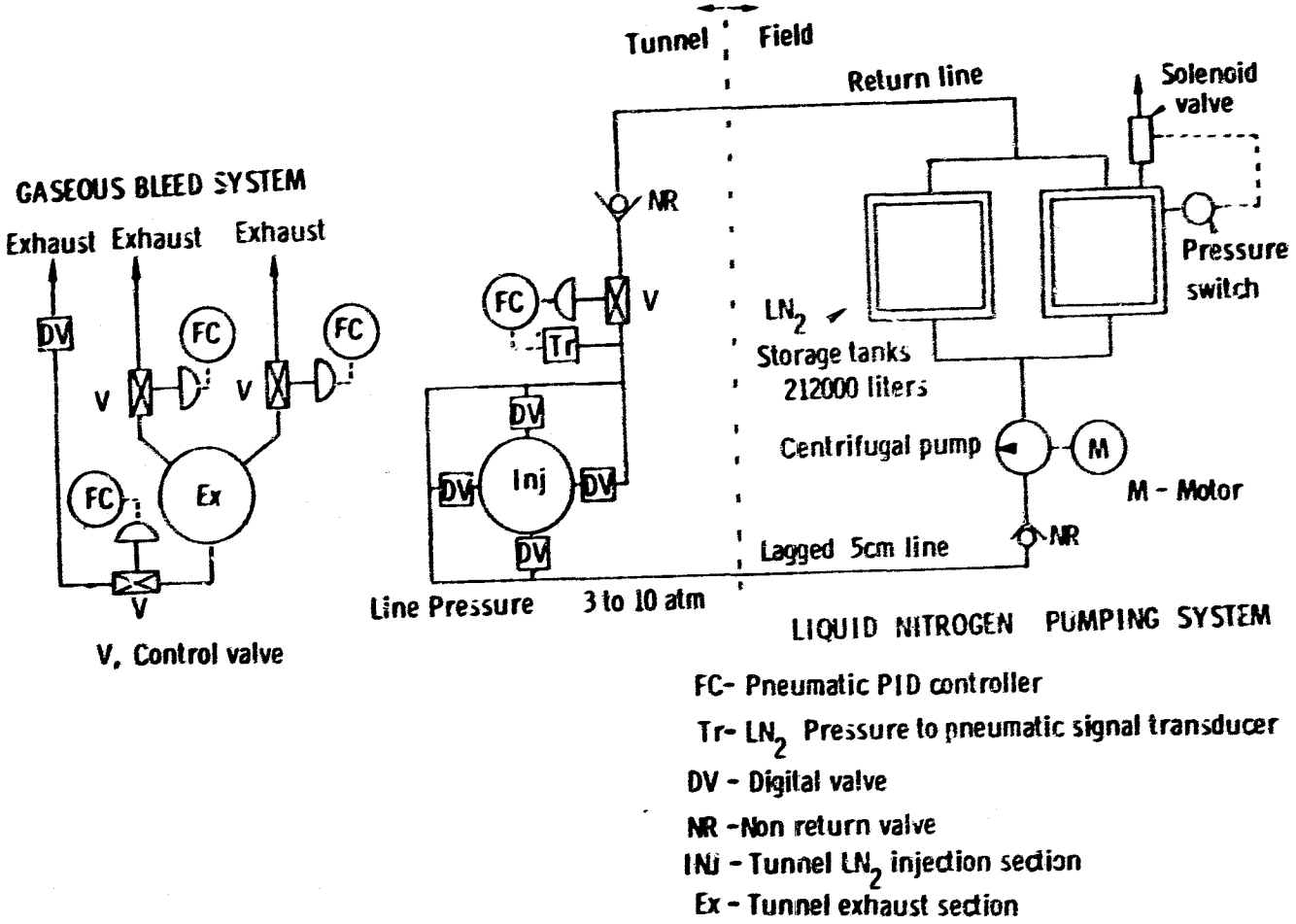

Figure 21. Liquid and gaseous nitrogen management schematic.

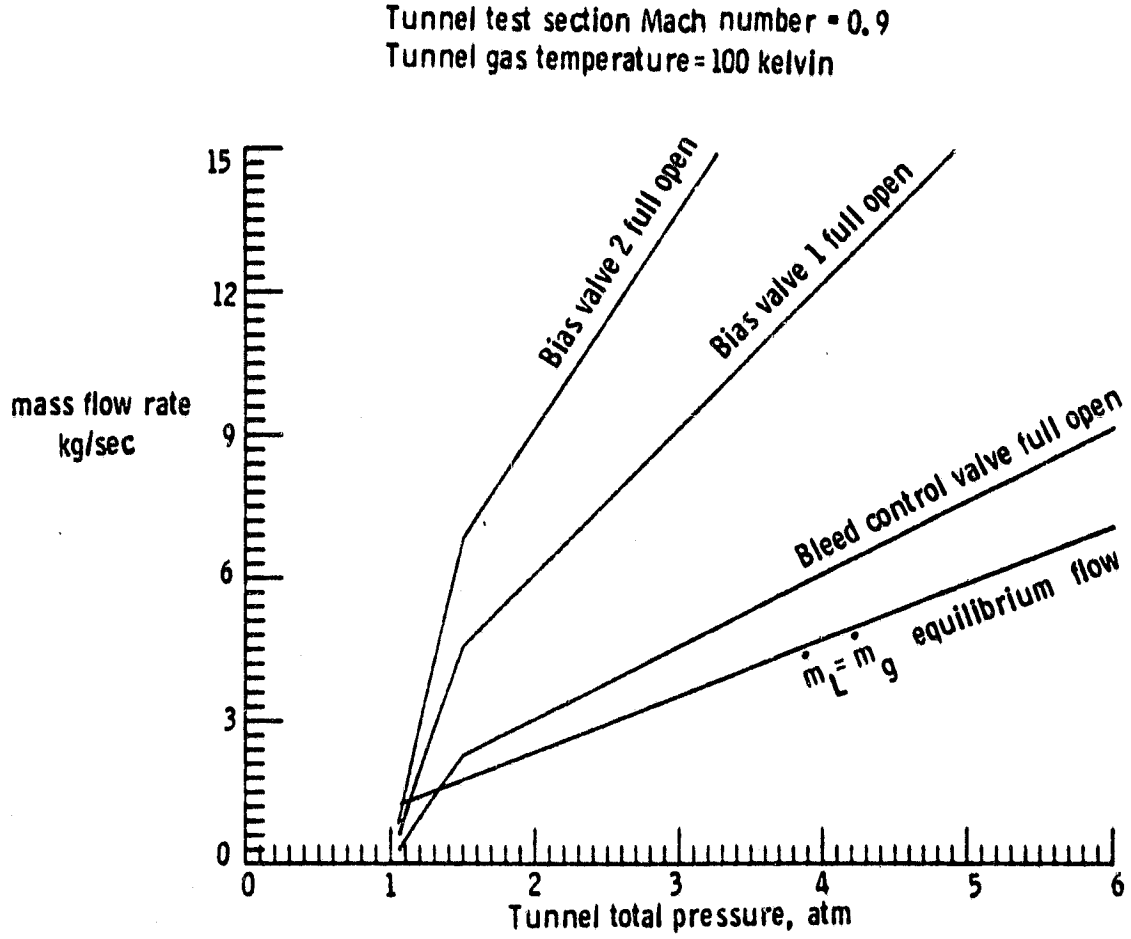

Figure 22. Gas bleed capability of tunnel pressure bleed valves at 100 K, M = 0.9.

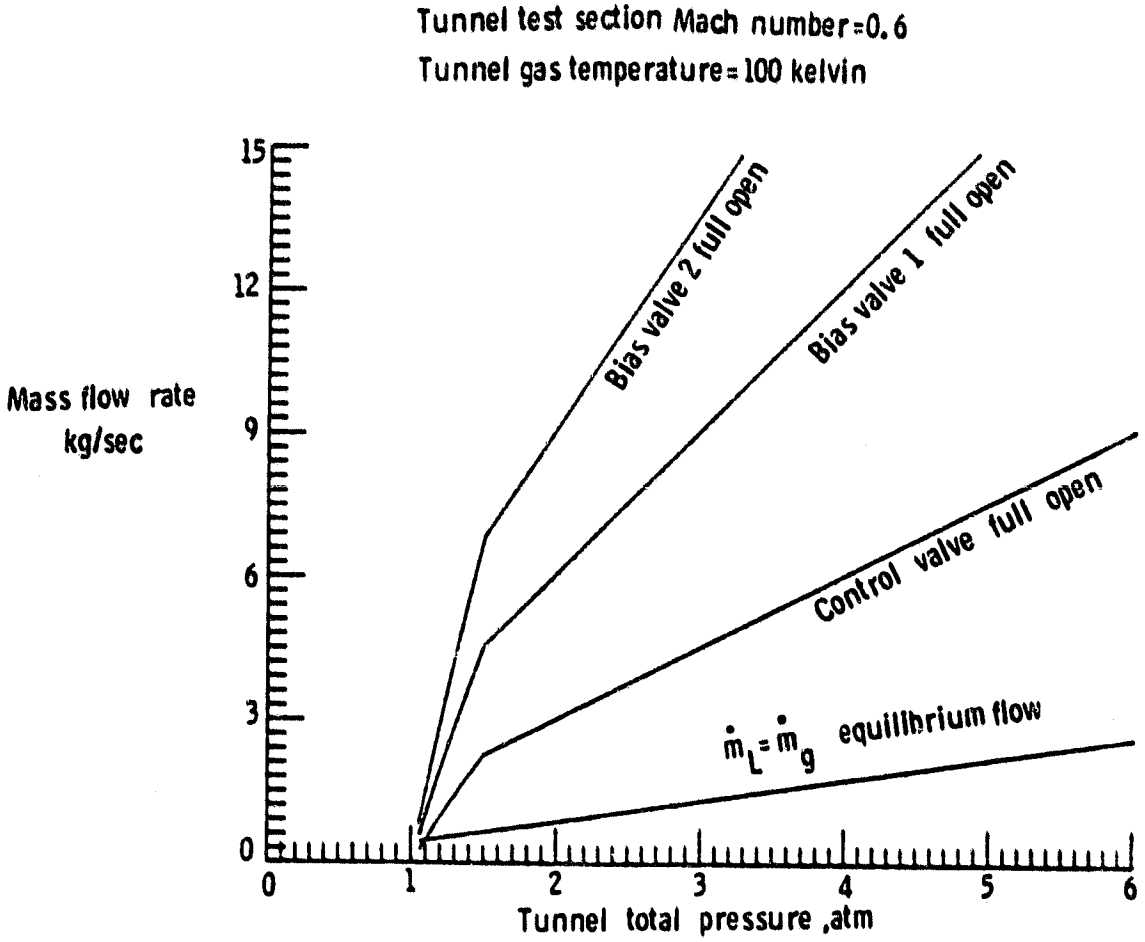

Figure 23. Gas bleed capability of tunnel pressure bleed valves at 100 K, M = 0.6

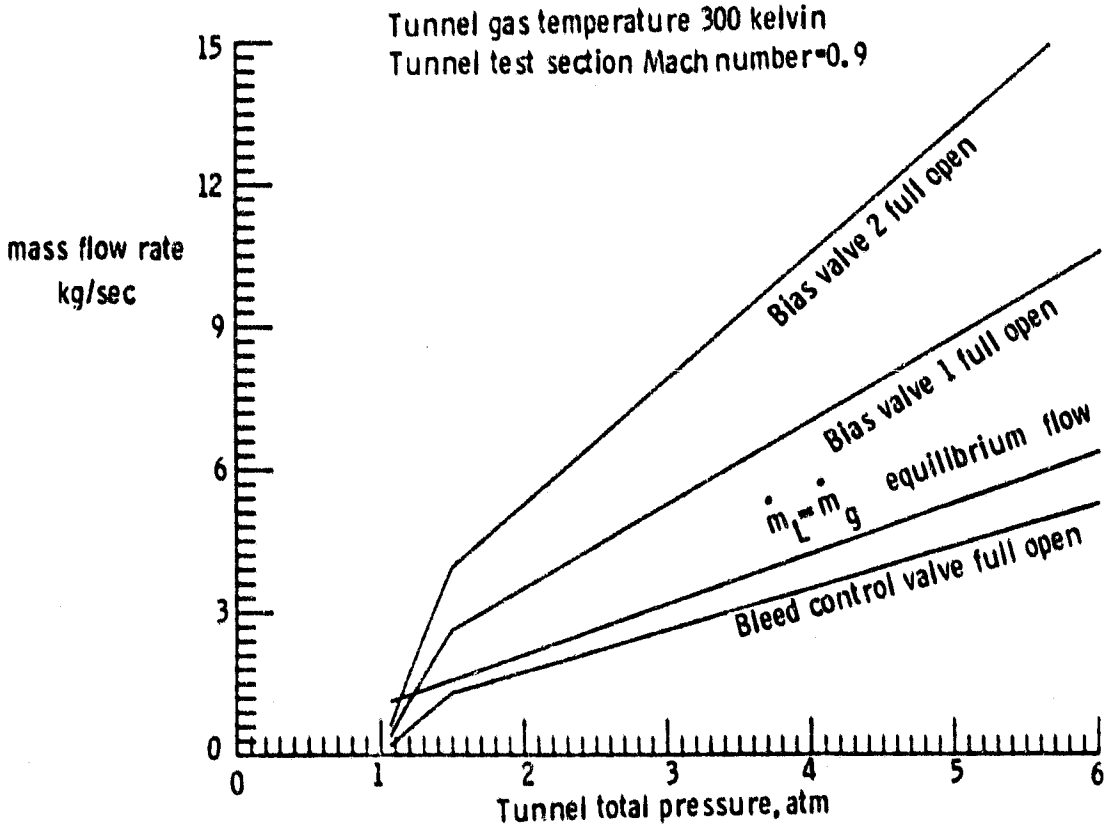

Figure 24. Gas bleed capability of tunnel pressure bleed valves at 300 K, M = 0.9.

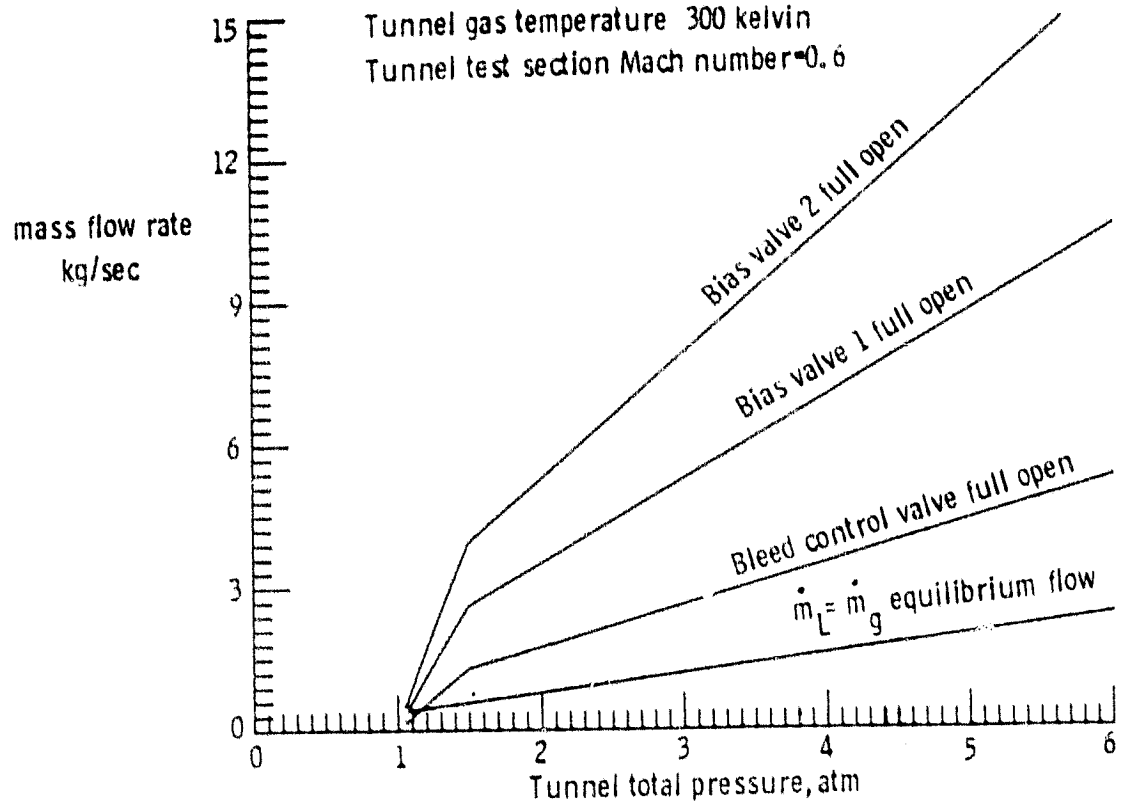

Figure 25. Gas bleed capability of tunnel pressure bleed valves at 300 K, M = 0.6.